การประยุกต์ใช้กระบวนการกลั่นแบบมีปฏิกิริยากับการผลิต เอทิล เทอร์เชียรี บิวทิล อีเทอร์ จาก เอทานอล และ เทอร์เชียรี บิวทานอล

นางสาว ดาริน วงศ์วัฒนะเศรษฐ์

วิทยานิพนธ์นี้เป็นส่วนหนึ่งของการศึกษาตามหลักสูตรปริญญาวิศวกรรมศาสตรมหาบัณฑิต
สาขาวิชาวิศวกรรมเคมี ภาควิชาวิศวกรรมเคมี
คณะวิศวกรรมศาสตร์ จุฬาลงกรณ์มหาวิทยาลัย
ปีการศึกษา 2545

ISBN 974-17-9894-6

APPLICATION OF REACTIVE DISTILLATION FOR PRODUCTION OF ETHYL TERTIARY BUTYL ETHER FROM ETHANOL AND TERTIARY BUTANOL

Miss Darin Wongwattanasat

A Thesis Submitted in Partial Fulfillment of the Requirements
for the Degree of Master of Engineering in Chemical Engineering
Department of Chemical Engineering
Faculty of Engineering
Chulalongkorn University
Academic Year 2002

ISBN 974-17-9894-6

Thesis Title	APPLICATION OF REACTIVE DISTILLATION FOR PRODUCTION OF ETHYL TERTIARY BUTYL ETHER FROM ETHANOL AND TERTIARY BUTANOL
By	Miss Darin Wongwattanasat
Field of Study	Chemical Engineering
Thesis Advisor	Associate Professor Suttichai Assabumrungrat, Ph.D.

Accepted by the Faculty of Engineering, Chulalongkorn University in Partial Fulfillment of the Requirements for the Master's Degree

….……. Dean of Faculty of Engineering
(Professor Somsak Panyakeow, D.Eng.)

THESIS COMMITTEE

…….. Chairman
(Associate Professor Ura Pancharoen, D.Eng.Sc.)

…….. Thesis Advisor
(Associate Professor Suttichai Assabumrungrat, Ph.D.)

……... Member
(Associate Professor Tharathon Mongkhonsi, Ph.D.)

…….. Member
(Assistant Professor Prasert Pavasant, Ph.D.)

ดาริน วงศ์วัฒนะเศรษฐ์: การประยุกต์ใช้กระบวนการกลั่นแบบมีปฏิกิริยากับการผลิตเอทิล เทอร์เชียรี บิวทิล อีเทอร์ จาก เอทานอล และ เทอร์เชียรี บิวทานอล (APPLICATION OF REACTIVE DISTILLATION FOR PRODUCTION OF ETHYL TERTIARY BUTYL ETHER FROM ETHANOL AND TERTIARY BUTANOL) อ. ที่ปรึกษา : รศ.ดร.สุทธิชัย อัสสะบำรุงรัตน์, 82 หน้า, ISBN 974-17-9894-6

วิทยานิพนธ์นี้เกี่ยวข้องกับการสังเคราะห์เอทิล เทอร์เชียรี บิวทิล อีเทอร์ (ETBE) ในสถานะของเหลว จากเอทานอล (EtOH) และเทอร์เชียรี บิวทานอล (TBA) โดยใช้ตัวเร่งปฏิกิริยาซีโอไลต์เบตา ที่ถูกสังเคราะห์ขึ้น โดยมีค่าอัตราส่วน Si/Al เท่ากับ 36 และที่มีใช้อยู่ในทางการค้า ซึ่งมีค่าอัตราส่วน Si/Al เท่ากับ 13.5 และ 55 จากการศึกษาตัวเร่งปฏิกิริยาซีโอไลต์เบตาที่มีค่าอัตราส่วน Si/Al ที่ต่างกันทั้ง 3 ค่า พบว่าให้ค่าการเปลี่ยนและค่าการเลือกเกิดใกล้เคียงกัน อย่างไรก็ตาม ตัวเร่งปฏิกิริยาที่มีค่าอัตราส่วน Si/Al เท่ากับ 55 ได้ถูกนำมาใช้ในการทดลองลำดับต่อไป ทั้งนี้เนื่องจากที่อัตราส่วนของ Si/Al ค่านี้สามารถหาได้ทางการค้า และ อยู่ในรูปแบบที่สามารถใช้งานได้ทันที ในการศึกษาจลนพลศาสตร์และกระบวนการกลั่นแบบมีปฏิกิริยา ซีโอไลต์เบตาที่มีอัตราส่วน Si/Al เท่ากับ 55 ถูกนำมาเคลือบบนโมโนลิท ใช้เป็นตัวเร่งปฏิกิริยาในเครื่องปฏิกรณ์แบบกึ่งกะ ในช่วงอุณหภูมิการทดลอง 343-363 K เพื่อหาค่าคงที่ของอัตราการเกิดปฏิกิริยาจากสมการอาร์เรเนียสและสัมประสิทธิ์การยับยั้งปฏิกิริยาโดยน้ำจากสมการของแวนท์ฮอฟ

การศึกษาระบบการกลั่นแบบมีปฏิกิริยา เบดของตัวเร่งปฏิกิริยาถูกบรรจุอยู่ที่ส่วนกลางของหอกลั่น โดยมีวัสดุสำหรับบรรจุในหอกลั่นที่ทำจากตะแกรงลวดเหล็กกล้าไร้สนิม บรรจุอยู่ส่วนบนและส่วนล่างของหอกลั่น ผลการดำเนินการที่สภาวะมาตรฐานพบว่าค่าการเปลี่ยนและค่าการเลือกเกิด เท่ากับร้อยละ 60.5 และร้อยละ 27.7 ตามลำดับ นอกจากนี้ยังได้ศึกษาถึงผลของสภาวะการดำเนินการต่าง ๆ คือ อุณหภูมิของเครื่องควบแน่น อัตราการป้อนของสารตั้งต้น อัตราส่วนการป้อนกลับ อัตราการให้พลังงานความร้อน และอัตราส่วนโดยโมลของเอทานอล:น้ำ ในสายป้อน โดยใช้โปรแกรม Aspen Plus

ภาควิชา..... วิศวกรรมเคมี ..... ลายมือชื่อนิสิต.....

สาขาวิชา..... วิศวกรรมเคมี ..... ลายมือชื่ออาจารย์ที่ปรึกษา.....

ปีการศึกษา..... 2545 .....

4370296321 : MAJOR CHEMICAL ENGINEERING
KEY WORDS : REACTIVE DISTILLATION, SIMULATION, ETBE synthesis, Beta zeolite, TBA

DARIN WONGWATTANASAT : APPLICATION OF REACTIVE DISTILLATION FOR PRODUCTION OF ETHYL TERTIARY BUTYL ETHER FROM ETHANOL AND TERTIARY BUTANOL. THESIS ADVISOR: ASSOC. PROF. SUTTICHAI ASSABUMRUNGRAT, Ph.D. 82 pp., ISBN 974-17-9894-6

This thesis concerns with the synthesis of ethyl *tert*-butyl ether (ETBE) from the liquid phase reaction between ethanol (EtOH) and *tert*-butyl alcohol (TBA) by using synthesized beta zeolite with Si/Al ratio of 36 and commercial beta zeolite with Si/Al ratio of 13.5 and 55. It was found that all beta zeolites with different Si/Al ratio offer almost the same conversion and selectivity of ETBE. However, the beta zeolite with the Si/Al ratio of 55 was selected for the following studies, as it was available in commercial market and present in a ready-to-use form. Beta zeolite supported on monolith was used in the kinetic and reactive distillation studies,. The reaction was carried out in a semi-batch reactor in the temperature range of 343-363 K to obtain the parameters of the reaction rate constant and the water inhibition coefficient.

In the reactive distillation study, the supported beta zeolite was placed in the middle of the column and stainless steel packing material was used in the top and the bottom sections of the column. Results under the standard operating condition indicated that the conversion and the selectivity were 60.5 and 27.7%, respectively. In addition, various operating parameters such as condenser temperature, total molar feed flow rate, reflux ratio, heat duty and mole ratio of H_2O:EtOH were simulated to find the effects on the reactive distillation performance by using Aspen Plus.

Department…..Chemical Engineering… Student's signature ……...
Field of Study..Chemical Engineering… Advisor's signature……...
Academic year…….2002……

ACKNOWLEDGEMENT

The author would like to express her greatest gratitude to her advisor, Associate Professor Suttichai Assabumrungrat, for his advice, help, suggestions and teaching the way to be good in study, research and chemical engineering. His kind suggestions motivated the author with strength and happiness to do this thesis. Although this thesis had obstacles, finally it could be completed by his advice. In addition, I would also grateful to Associate Professor Ura Pancharoen, as the chairman and Associate Professor Tharathon Mongkhonsi and Assistant Professor Prasert Pavasant, as the members of the thesis committee.

The author also had the thankfulness to Mr. Worapon Kiatkittipong, Miss Nisakorn Sriwithun, Mr. Choowong Chaisuk and many best friends in Chemical Engineering department who have provided encouragement and co-operate along the thesis study.

Moreover, the author would like to thank the Thailand Research Fund and TJTTP-OECF for gratefully acknowledged and financial support. Finally, she also would like to dedicate this thesis to her parents who have always been the source of her support and encouragement.

CONTENTS

page

CONTENTS (CONT.)

CONTENT (CONT.)

LIST OF TABLES

TABLE **page**

LIST OF FIGURES

FIGURE **page**

LIST OF FIGURES (CONT.)

FIGURE **page**

NOMENCLATURE

a_i	activity of species i	[-]
γ_i	activity coefficient of species i	[-]
c_i	concentration of species i	[mol/m^3]
D	total distillate flow	[mol/s]
F	feed flow rate	[mol/s]
k_{1a}	reaction rate constant of reaction (5.1)	
	in the activity-based model	[mol/(kg.s)]
k_{1c}	reaction rate constant of reaction (5.1)	
	in the concentration-based model	[m^6/(mol.kg.s)]
k_{2a}	reaction rate constant of reaction (5.2)	
	in the activity-based model	[mol/(kg.s)]
k_{2c}	reaction rate constant of reaction (5.2)	
	in the concentration-based model	[m^3/(kg.s)]
K_{1a}	equilibrium constant of reaction (5.1)	
	in the activity-based model	[-]
K_{1c}	equilibrium constant of reaction (5.1)	
	in the concentration-based model	[-]
K_{Wa}	water inhibition parameter	
	in the activity-based model	[-]
K_{Wc}	water inhibition parameter	
	in the concentration-based model	[m^3/mol]
m_i	number of mole of species i	[mol]
r_j	reaction rate of reaction j	[mol/(kg.s)]
R	gas constant (=8.314 J/mol)	[J/mol]
S_{ETBE}	selectivity of ETBE	[-]
T	temperature	[K]
Tc	the condenser temperature	[K]
x_i	mole fraction of species i in liquid mixture	[-]
X_{TBA}	conversion of TBA	[-]

Subscript

ETBE	ethyl *tert*-butyl ether
EtOH	ethanol
H_2O	water
IB	isobutylene
TBA	*tert*-butyl alcohol
o	initial value at $t = 0$

CHAPTER 1

INTRODUCTION

Over the past two decades, oxygenates have been used to increase the volume and octane of gasoline. In the late 1970s and early 1980s, as lead compounds were removed from gasoline, gasoline producer used oxygenates to offset the loss in octane from the removal of lead compounds. More recently, oxygenates have been used as an emission control strategy to reduce carbon monoxide (CO) and, to a lesser extent, hydrocarbon emission from motor vehicles. However, oxygenates can generally increase emissions of oxides of nitrogen (NO_x). Therefore the oxygen content in the gasoline for automobile engines have been limited to control NO_x emission.

There are several oxygenates that can be used to meet oxygen requirements into gasoline. They are divided into alcohols and ethers such as methanol (MeOH), ethanol (EtOH), methyl tertiary butyl ether (MTBE) and ethyl tertiary butyl ether (ETBE), etc. Currently, MTBE is used as a non-toxic octane enhancer in the reformulated gasoline instead of lead compounds. However, there is pending legislation in a number of states in the United State banning MTBE because it is soluble in water and has tendency to pollute underground water. MTBE is also not good in an environmental point of view because this is mostly derived from natural gas and may contribute further to global warming. The refiners are now facing with a big question of what oxygenate to replace MTBE to meet the required reformulated gasoline standard.

In addition to MTBE, the demand for ETBE has rapidly increased in recent years. The reasons as follows: (Yang *et al.*, 2000)

1. ETBE has a higher octane number (111) than MTBE (109) and lower vapor pressure (4 psi) than MTBE (8-10 psi).

2. EtOH, one of the starting materials for ETBE, can be produced from renewable sources such as cellulose, biomass or other farm products.

Most reports about the production of ETBE have focused on the method of liquid phase synthesis from EtOH and isobutylene (IB). However, an IB source is only limited to catalytic cracking or steam cracking fractions. IB is also used as a starting material in other chemical industries but cannot meet an increasing demand of *tert*-ethers. Since *tert*-butyl alcohol (TBA) is a major by-product in the ARCO process for the manufacture of propylene oxide (Matouq and Goto, 1993), it can provide an alternative route for the synthesis of ETBE. There are two routes to produce ETBE from TBA. In the indirect method, TBA is dehydrated to IB in the first reactor and then the produced IB reacts with EtOH to produce ETBE in the second reactor. In the direct method, TBA and EtOH react directly to form ETBE in one reactor.

Various catalysts have been tested for the direct route. They are homogeneous catalysts such as sulfuric acid and heterogeneous catalysts such as acidic ion exchange resins and acidic zeolites. Because of the reactive sensitivity of homogeneous catalysts with the present of water in feed and difficultly separated from solution and continuous operation are proceed, hence, focused on heterogeneous catalysts for example, Amberlyst-15 (Quitain *et al*., 1999a), heteropoly acid (Yin *et al*., 1995), potassium hydrogen sulphate (Matouq *et al*., 1996), S-54 and D-72 (Yang *et al*., 2000) and beta zeolite (Assabumrungrat *et al*., 2002). It is obvious that beta zeolite is a good shape selectivity catalyst, consequently, high selectivity and tolerant in thermal and high temperature conditions.

Reactive distillation (RD) is a combination of reaction and separation in the same process unit. The most important advantage of RD is for equilibrium-controlled reactions. RD can eliminate conversion limitations by continuous removal of products from the reaction zone. Examples of reactions are such as production of fuel ethers and esterification reactions. However, only a few studies apply the concept of reactive distillation to this direct synthesis route of ETBE production. (Yang and Goto, 1997 and Quitain *et al*., 1999a and 1999b). Some works also included a pervaporation unit in the reactive distillation column. The pervaporation unit was used for removing water in the bottom product of the column and resulting in almost doubling of the

mole fraction of ETBE in the top product. (Matouq *et.al.,* 1994 and Yang and Goto 1997). Later there are a number of works on using commercial software such as Aspen Plus, ProII and Speed up , etc to optimize plate performance, profitability and scale up in an industrial process. Quitain and coworker (1999a and b) proposed a process for synthesizing ETBE by using Aspen Plus simulator. As a result Aspen Plus has also been performed, good agreement between experimental and the simulation results being achieved. Various systems have been investigated. They are, for example, synthesis of butylacetate (Smejkal, 1998 and Hanika *et al.*, 1999), 2-Methylpropylacetace (Smejkal *et al.*, 2001) and liquid – liquid equilibria of of ternary 2M1B-2M2B-H_2O and quaternary 2M1B-2M2B-2M1BOH-H_2O mixture (Aiouache and Goto, 2001).

In this study, the direct synthesis of ETBE from TBA and EtOH in reactive distillation was investigated. The performances of synthesized beta zeolite with Si/Al ratio of 36 and commercial beta zeolites with Si/Al ratio of 13.5 and 55 were compared through a reaction in a semi-batch reactor. The kinetic parameters of the best catalyst supported on monolith were determined at a temperature range of 323-343 K. Experiments of the direct synthesis of ETBE were studied using a RD column packed supported beta zeolite bed. Finally the simulation studies were carried out using Aspen Plus, to investigate various operating conditions such as the condenser temperature, total feed molar flow rate, reflux ratio, heat duty and mole ratio of H_2O:EtOH on the RD performance.

CHAPTER 2

THEORY

2.1 Oxygenates

Oxygenates are compounds containing oxygen in a chain of carbon and hydrocarbon atoms. They can not provide energy, but their structure provides a reasonable anti-knock value, thus they are good substitutes for aromatics, and they may also reduce the smog-forming tendencies of the exhaust gases. Most oxygenates used in gasolines are either alcohols (C_x-O-H) or ethers (C_x-O-C_y), and contain 1 to 6 carbons. Alcohols have been used in gasolines since the 1930s while MTBE was first used in commercial gasoline in Italy in 1973 and in the US by ARCO in 1979. Over 95% of gasoline used in California were blended with MTBE in 1996. They can be produced from fossil fuels such as methanol (MeOH), methyl tertiary butyl ether (MTBE), tertiary amyl methyl ether (TAME), or from biomass, such as ethanol (EtOH), ethyl tertiary butyl ether (ETBE). Oxygenates have significantly different physical properties compared to hydrocarbons as shown in Table 2.1, and the levels that can be added to gasolines are controlled by the EPA in the US, with waivers being granted for some combinations. Initially the oxygenates were added to hydrocarbon fractions that were slightly-modified unleaded gasoline fraction, and these were commonly known as “oxygenated” gasolines. In 1995, the hydrocarbon fraction was significantly modified, and these gasolines are called “reformulated gasolines” (RFGs). The change to reformulated gasoline requires oxygenates to provide octane, but also that the hydrocarbon composition of RFG must be significantly more modified than the existing oxygenated gasolines to reduce degree of unsaturation, volatility, benzene, and the reactivity of emissions. Oxygenates are beneficial to gasoline function in two ways. Firstly they have high blending octane, and so can replace high octane aromatics in the fuel. These aromatics are responsible for disproportionate amounts of CO and HC exhaust emissions. This is called the “aromatic substitution effect”. Oxygenates also cause engines without sophisticated engine management systems to move to the lean side of stoichiometry, thus reducing emission of CO (2% oxygen can reduce CO by 16%) and HC (2% oxygen can reduce

HC by 10%). However, on vehicles with engine management systems, the fuel volume will be increased to bring the stoichiometry back to the preferred optimum setting. Oxygen in the fuel can not contribute energy and consequently the fuel has less energy content. For the same efficiency and power output, more fuel has to be burnt, and the slight improvements in combustion efficiency that oxygenates provide on some engines usually do not completely compensate for the oxygen.

Table 2.1 Physical properties of oxygenates

	Motor Octane Number	Research Octane Number	Reid Vapour Pressure (kPa)	Boiling Point (K)	Water Tolerance
Ethers					
MTBE	101	118	55	328	Excellent
ETBE	102	118	28	345	Excellent
TAME	99	109	10	359	Excellent
Alcohols					
MeOH	92	107	32.1	338	Poor
EtOH	96	130	124.1	351	Very poor
TBA	95	105	48.1	344	Poor
Gasoline	82-88	92-98	70-100	299-503	N/A

2.1.1 ETBE

Generally, ETBE can be produced by an exothermic reversible reaction between EtOH and isobutene (IB). However, the supply of IB which is mainly obtained from refinery catalytic cracking and steam cracking fractions becomes limited due to the increased demand of MTBE and ETBE. Hence, alternative routes for the synthesis of ETBE are currently explored. Tertiary butyl alcohol (TBA) which is a major byproduct of propylene oxide production from isobutane and propylene, can be employed instead of IB as a reactant.

Two ways to produce ETBE can be considered, those are, indirect and direct methods. In the indirect methods, TBA is dehydrated to IB in a first reactor and then the produced IB reacts with EtOH to produce ETBE in a second reactor. In the direct method, ETBE can be produced directly from TBA and EtOH in one reactor. This process is favorable not only because it shortens the process itself, but also because it would reduce demand to the purity of EtOH. Since the reaction itself produces water, the content of water in EtOH becomes insignificant.

ETBE could possibly be used as an oxygenate to replace MTBE due to the follow reasons:

- Production processes similar to MTBE, minor refinery retooling
- Higher octane number than MTBE
- Lower RVP (Reid Vapor Pressure) & solubility in water than MTBE
- More biodegradable than MTBE
- Can be blended at refinery and transported through pipelines
- Eligible for tax credits (not if added at refinery)
- Comparable blends need 15% more ETBE than MTBE

2.2 Zeolite

Zeolites are crystalline aluminosilicates with fully cross-linked open framework structures made up of corner-sharing SiO_4 and AlO_4 tetrahedra. The first zeolite, stibnite, was discovered by Cronstedt in 1756, who found that the mineral loses water rapidly on heating and thus seems to boil. The name “Zeolite” comes from the Greek words zeo (to boil) and lithos (stone). A representative empirical formula of zeolite is $M_{2/n}.Al_2O_3.xSiO_2.yH_2O$, where M represents the exchangeable cation of valence n. M is generally a group I or II ion, although other metal, non-metal and organic cations may also balance the negative charge created by the presence of Al in the structure. The framework may contain cages and channels of discrete size, which are normally occupied by water.

In addition to Si^{4+} and Al^{3+}, other elements can also be present in the zeolitic framework. They need not be isoelectronic with Si^{4+} and Al^{3+}, but must be able to occupy framework sites. Aluminosilicate zeolites display a net negative framework charge.

2.2.1 Structure of Zeolite

The framework of a zeolite is based on an extensive three-dimensional network in which the polyhedral sites, usually tetrahedral, are linked by oxygen atoms. The crystalline framework contains cages and channels of discrete size and 3-30^{o}A in diameter. The primary building unit of a zeolite is the individual tetrahedral unit. The T atom (T = Si or Al) belonging to a TO_4 tetrahedron is located at each corner, but the oxygens located near the mid-points of the lines joining each pair of T atoms.The topology of all known zeolite framework types can be described in terms of a finite number of specific combinations of tetrahedral called “secondary building units”(SBU’s). A zeolite framework is made up of one type of SBU only.

Description of the framework topology of a zeolite involves “tertiary” building units corresponding to different arrangements of the SBU’s in space. Various alternative ways have been proposed. The framework may be considered in terms of large polyhedral building blocks forming characteristic cages. For example, sodalite, zeolite A and zeolite Y can all be generated by the truncated octahedron known as the beta-cage. An alternative method of describing extended structures uses two-dimensional sheet building units. Sometimes various kinds of chains can be used as the basis for constructing a zeolite framework.

2.2.2 Properties of Zeolite

The most important application of zeolite is as a catalyst. Zeolites combine high acidity with shape selectivity, high surface area, high thermal stability and have been used to catalyze a variety of hydrocarbon reactions, such as cracking, hydrocracking, alkylation and isomerisation. The reactivity and selectivity of zeolites as catalysts are determined by the active sites brought about by a charge imbalance between the silicon and aluminium atoms in the framework. Each framework

aluminium atom induces a potential active acid site. In addition, purely siliceous and $AlPO_4$ molecular sieves have Brønsted acid sites whose weak acidity seems to be caused by the presence of terminal OH bonds on the external surface of crystal.

Shape selectivity, including reactant shape selectivity, product shape selectivity or intermedia shape selectivity plays a very important role in zeolite catalysis. The channels and cages in a zeolite are similar in size to medium-sized molecules. Different sizes of channels and cages may therefore promote the diffusion of different reactants, products or intermedia species. High crystallinity and the regular channel structure are the principal features of zeolite catalysts. Reactant shape selectivity results from the limited diffusivity of some of the reactants, which can not effectively enter and diffuse inside the crystal. Product shape selectivity occurs when slowly diffusing product molecules can not rapidly escape from the crystal, and undergo secondary reactions. Restricted intermedia shape selectivity is a kinetic effect arising from the local environment around the active site: the rate constant for a certain reaction mechanism is reduced if the necessary intermedia is too bulky to form readily.

Zeolites are selective, high-capacity adsorbents because of their high intracrystalline surface area and strong interactions with adsorbates. Molecules of different size generally have different diffusion properties in the same molecular sieve. Molecules are separated on the basis of size and structure relative to the size and geometry of the apertures of zeolite. Zeolites adsorb molecules, in particular those with a permanent dipole moments, and exhibit other interactions not found in other adsorbents. Different polar molecules have a different interaction with the zeolite framework, and may thus be separated by a particular zeolite. This is one of the major uses of zeolites. An example is the separation of N_2 and O_2 in the air on zeolite A, by exploiting different polarities of the two molecules.

Zeolites with low Si/Al ratios have strongly polar anionic frameworks. The exchangeable cation creates strong local electrostatic fields and interacts with highly polar molecules such as water. The cation-exchange behaviour of zeolites depends on (1) the nature of the cation species - the cation size (both anhydrous and hydrated) and cation charge, (2) the temperature, (3) the concentration of the cationic species in the

solution, (4) the anion associated with the cation in solution, (5) the solvent (most exchange has been carried out in aqueous solutions, although some work has been done in organics) and (6) the structural characteristics of the particular zeolite.

2.2.3 Solid Heterogeneous Catalyst: Beta Zeolite

Beta zeolite is an old zeolite discovered before Mobil began the “ZSM” naming sequence. As the name implies, it was the second in an earlier sequence. Beta zeolite was initially synthesized by Wadlinger *et al*.(1995) using tetraethylammonium hydroxide as an organic template.

The chemical composition of beta zeolite is:
$(TAE,Na)_2O.Al_2O_3.5\text{-}100SiO_2.4H_2O$

Beta zeolite is a large pore, high silica, crystalline aluminosilicate. The framework and the pore structure of the zeolite have several unique feature. It is the only large pore zeolite to have chiral pore interactios. The high silica zeolites are attractive catalytic materials because of their thermal and hydrothermal stabilities, acid strength, good resistance for deactivation and hydrophobicity. The pore structure of beta zeolite consists of 12 membered rings interconnected by cages formed by the interaction of channels. The dimension of pore opening in the linear channel is 5.7 ^{o}A x7.5 ^{o}A. The tortuous channel system consists of the interactions of two linear channels of approximate dimensions of 5.6 ^{o}A x 6.5 ^{o}A. Beta zeolite has a total pore volume around 0.2 ml/g. The above characteristics make beta zeolite a potential candidate for a variety of hydrocarbon conversion reactions. The framework structures of beta zeolite are shown in Figure 2.1.

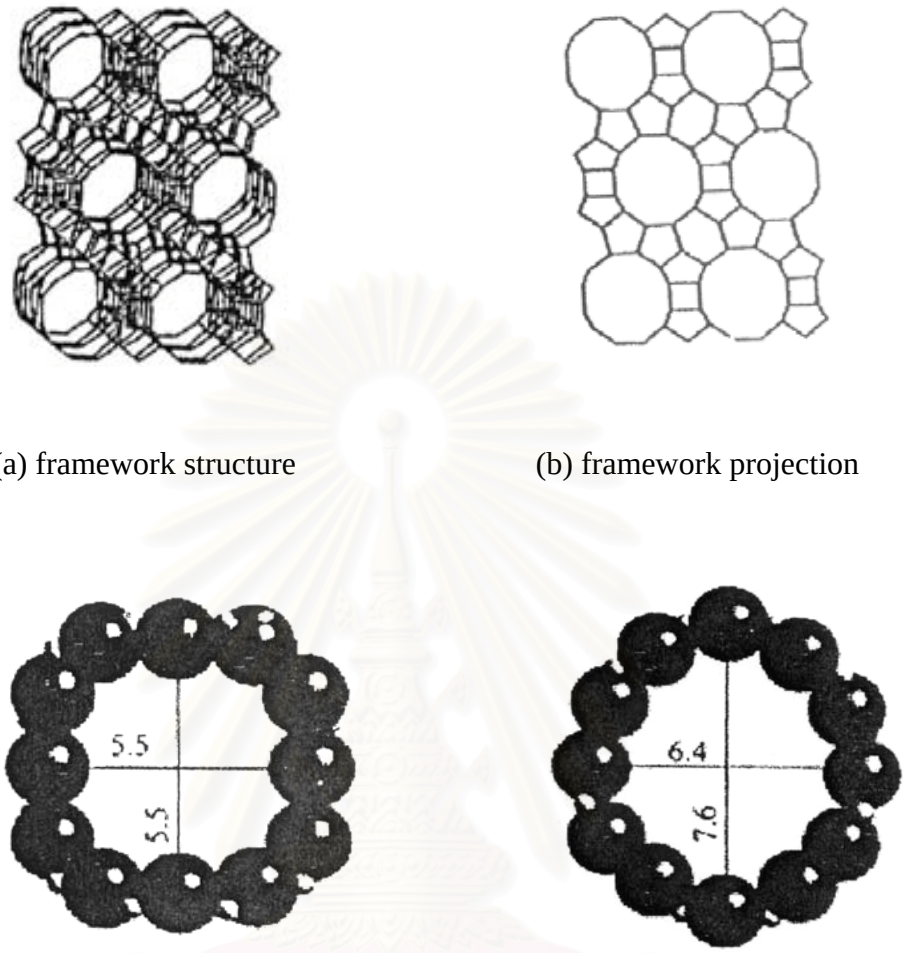

(a) framework structure (b) framework projection

(c) tortous channel (d) straight channel

Figure 2.1 Structure of beta zeolite

2.2.4 Catalyst Support : Monolith

At Delft University of technology, technology has been developed to prepare binderless films of catalytically active zeolite crystals on metal and ceramic supports. In short, the preparation procedure consists of immersing the support structure in an aqueous solution containing the reactants for zeolite synthesis, after which the system is heated and zeolite crystals grow on the surface of the support (Oudshoorn *et al*., 1999).

However, the commercial ceramic supports, ceramic monoliths, have large pores and low surface areas, so it is necessary to deposit a high surface area carrier, which is subsequently catalyzed, onto the channel wall. The catalyzed coating is composed of a high surface area material such as Al_2O_3 which will be subsequently impregnated with a catalytic component such as Pt. This is referred as the catalyzed wash coat, illustrated in Figure 2.2. The wash coat depends primarily on the geometry of the channel and the coating method. The pollutant-containing gases enter the channels uniformly and diffuse to the catalytic sites where they are converted catalytically to harmless products.

Monoliths offer a number of design advantages that have led to their widespread use in environmental applications such as catalytic converter used for automotive emissions control. However, the most important advantage is the low pressure drop with high flow rates. The monolith which has a large open frontal area and with straight parallel channel offers less resistance to flow than that of pellet-type catalyst.

Monoliths are generally fabricated from ceramic or metal. The characteristics and properties of both types of monolith are described below.

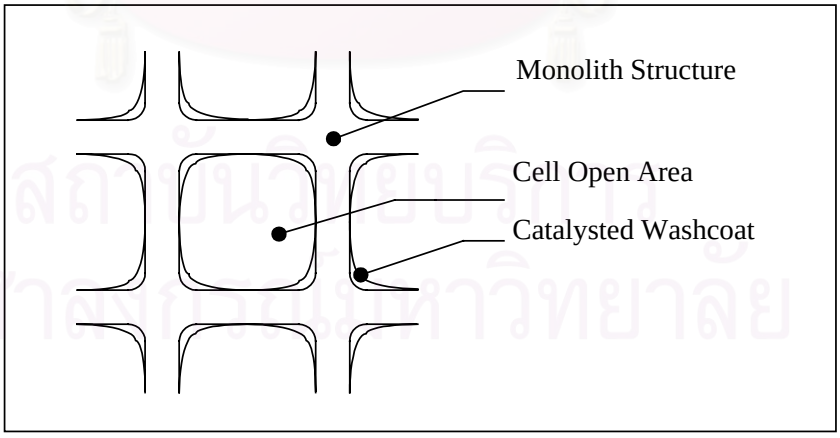

Figure 2.2 Ceramic monolith coated with a catalyzed wash coat

Ceramic monolithic supports are made of alumina and related materials such as cordierite ($Al_4Mg_2Si_5O_{18}$), mullite ($3Al_2O_3SiO_2)_2$, spoumene ($LiAl(SiO_3)_2$), and asbestos ($Mg_3(Si_2O5)_2(OH)$). Synthetic cordierite, the first mentioned above, is by far the most commonly used ceramic for monolithic catalyst support applications. Raw materials such as kaolin, talc, aluminium hydroxide, and silica are blended into a paste and extruded and calcined. It is possible to produce sizes up to about 27.94 cm in diameter and 17.78 cm long, with cell densities from 9 to 600 cells per square inch (cpsi). The conversion desired, the physical space available for the reactor, and engineering constraint such as pressure drop are considered when designing the monolith size.

Cordierite monolith posses several important properties that make this materials preferable for use as a support. These properties are described below.

Thermal shock resistance

By nature of its low thermal expansion coefficient ($10x10^{-7}$/K), cordierite undergoes little dimensional change when cycled over a wide temperature range. Thus, it resists cracking due to thermal shock.

The wash coat influences the thermal shock resistance of the monolith (especially during rapid temperature changes) because it expands more than the monolith. Particle size of the carrier and thickness of the wash coat are two key parameters that must be optimized.

Mechanical strength

Monoliths are made with axial strengths of approximately over 210 kg per square centimeter. They must be resistant to both axial and mechanical perturbations experience in automotive, truck, and aircraft applications. The high mechanical integrity is derived from the physical and chemical properties of the raw materials and the final processing after extrusion.

Melting point

The melting point of cordierite is over 1573 K far greater than temperature expected for modern environment applications. The materials are also resistant to harsh environmental such as high temperature, stream, sulfur oxides, oil additive constituents, that are present in many exhaust sources.

Catalyst compatibility

Automotive ceramic monolith has well-designed pore structure (approximate 3-4 micron) that allows good chemical and mechanical bonding to the wash coat. The chemical components in the ceramic are strongly immobilized, so little migration from the monolith into the catalyzed wash coat occurs.

Table 2.2 lists a representative selection of currently available ceramic monolith geometric. An increase in cell density from 100 to 300 cpsi (cell per square inch) significantly increases the geometric area from 157 to 260 cm^2/cm^3 but decreases the channel diameter from 0.21 to 0.12 cm. The wall of the ceramic drops in thickness from 0.04 to 0.03 cm.

Table 2.2 Physical properties of ceramic monolith.

Cell density (cpsi)	Hydraulic Channel Diameter (inches)	Open frontal Area (%)	Geometry surface area (ft^2/ft^3)	Pressure Drop (inches of H_2O)	Wall thickness (inches)
64	0.099	70	340	0.075	0.019
100	0.083	69	398	0.095	0.017
200	0.059	72	576	0.210	0.012
300	0.046	65	660	0.300	0.012
400	0.044	71	852	-	0.006

The increase in cell density causes an increase in pressure drop at a given flow rate. For example, a flow rate of 300 standard cubic feet per minute (SCFM) (8.4x106 cm^3/min.) through a monolith of 929 cm^2 by 2.54 cm thick, the pressure drop for a 100 cpsi is about 0.254 cm of water, compared to about 0.762 cm of water for a 300 cpsi monolith.

Metal supports, metal monoliths, made of high temperature resistant alumina-containing steels are catalyst supports which have found several applications, mainly because they can be prepared with thinner walls than a ceramic. This offers the potential for higher cell densities with lower pressure drop. The wall thickness of a 400 cpsi metal substrate used for automotive applications is only about 25 percent of its ceramic couterpart: 0.004-0.005 cm compared to 0.015-0.02 cm, respectively. The open frontal area of the ceramic with the same cell density. its thermal conductivity is also considerable higher (by about 15-20 times) than the ceramic, resulting in faster heat-up. This property is particularly important for oxidizing hydrocarbons and carbon monoxide emissions when a vehicle is cold. Metal substrates also offer some advantages for converter installations in that they can be welded directly into the exhaust system. A common design is that of corrugated sheets of metal welded or wrapped together into a monolithic structure.

Adhesive of the oxide based wash coat to the metallic surface and corrosion of the steel in high-temperature steam environmental were early problem that prevented their widespread used in all but some specialized automotive applications. Surface pretreatment of the metal has reduced the adherence problems, and new corrosion-resistant steel is allowing metal to slowly penetrate the automotive markets. They are currently used extensively for low-temperature applications such as NO_x in power plants, O_3 abatement in airplanes, CO and VOC abatement and (quite recently) catalytic converters for natural gas fueled vehicles. They are usually about twice as expensive as their ceramics counterpart.

2.3 Reactive Distillation

A chemical reaction and multistage distillation can be carried out simultaneously. The combined unit operation, called reactive distillation, especially suits those chemical reactions where reaction equilibrium limits the conversion in a conventional reactor to a low-to-moderate level. By continuously separating products from reactants while the reaction is in progress, the reaction can proceed to much higher level of conversion than otherwise possible.

The concept of reactive distillation is not new. The technique was first applied in the 1920's to esterification processes using homogeneous catalysts and was reviewed by Keyes in 1932. Implementation of the reactive distillation for reactions that rely on a solid heterogeneous catalyst is a more recent development.

2.3.1 Reactive Distillation Configurations

A conventional configuration for a process involving a catalytic chemical reaction with a solid catalyst involves two steps of chemical reaction and subsequent separation. In the chemical reaction step, reactants are brought into contact with solid catalysts at appropriate process conditions in one or more reactors. The stream leaving the reactor section then goes to one or more separation steps where unconverted reactants are separated from the products of the reaction and the inerts. The unconverted reactants, in some cases, may be recycled to the reaction section. When a substantial amount of inerts are present in the system, at least two separation units for separation of high purity product and for separation of the unconverted reactants from the inerts are required. The separation process typically chosen is distillation.

A conventional process configuration is shown in Figure 2.3. The separation process is distillation. In the case, a reaction product is less volatile than reactants and inert. The flow diagram of the application of reactive distillation to this process is shown in Figure 2.4. The middle section of the column is the reactive distillation section. For a non-azeotopic chemical system, separation of the inerts takes place in the rectification section of the column and the purification of the product takes place in the stripping section.

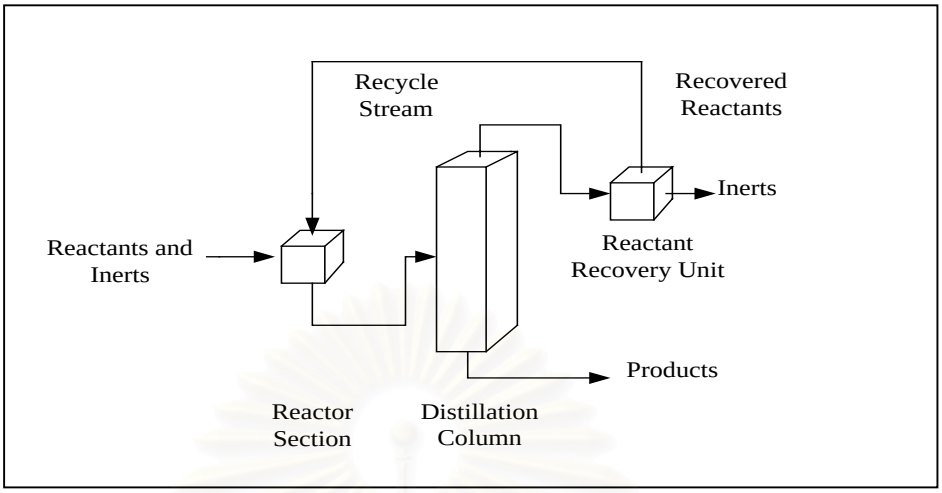

Figure 2.3 Conventional process involving reaction followed by separation

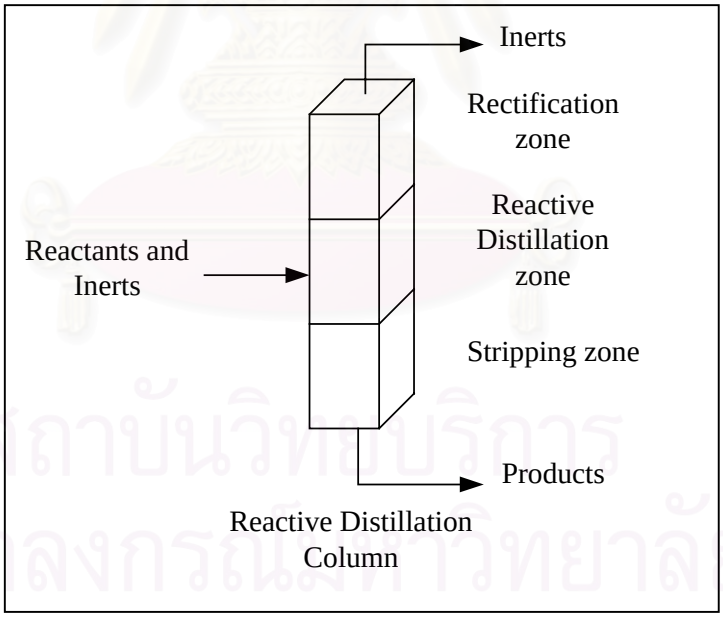

Figure 2.4 Reactive distillation applied to the same process

In the presence of a solid catalyst bed, the reactive distillation can be carried out in several different configurations. In one configuration, the solid-catalyzed chemical reaction and the multistage distillation occur simultaneously in a continuum that is, there is spatial continuity along the length of the column. Both reaction and distillation take place in every thin horizontal slice of the reactive distillation section of the column.

In the other configuration, the reaction and distillation proceed in alternating steps. Here, the reactive distillation section of a column contains both the catalyst contact device and the distillation device. A reaction occurs in the catalyst contact device and then the reacting phase passes to the distillation device for vapor/liquid contact and separation. These two steps occur alternately. By making the steps of infinitely small size, this configuration becomes equivalent to the first one.

In both configurations, a rectification section may be located above the reactive distillation section of the column and a stripping section may be located below it, depending upon purity specifications.

In some systems a combination, as shown in Figure 2.5, of the conventional process and reactive distillation may be optimal. Since part of the conversion is shifted to the reactive distillation column, the size of the fixed-bed reactor becomes smaller than in the conventional process, or the number of reactors may be decreased. The reactor effluent is the reactive distillation column feed and the remaining conversion takes place in the reactive distillation zone.

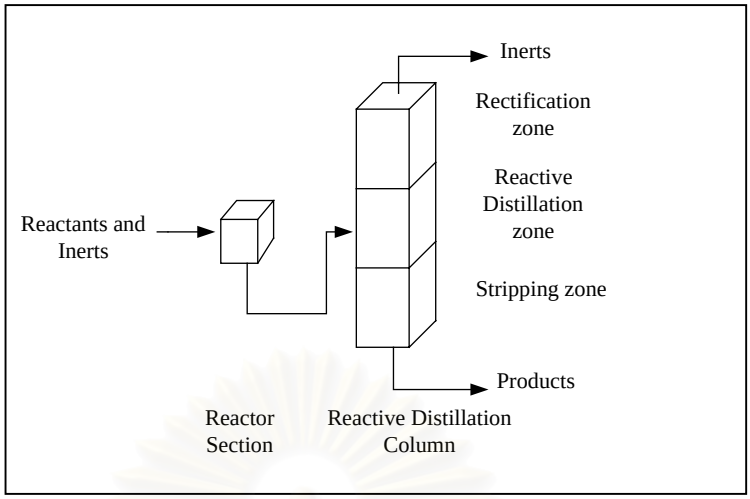

Figure 2.5 Combining reactive distillation with a conventional process offers

2.3.2 Advantages of Reactive Distillation

Application of RD to a catalytic chemical reaction using solid catalysts leads to a substantial cost savings compared to a conventional process. These savings result from :

- An important benefit of RD technology is a reduction in capital investment, because two process steps can be carried out in the same device. Such and integration leads to lower costs in pumps, piping and instrumentation.

- If RD is applied to exothermic reaction, the reaction heat can be used for vaporization of liquid. This leads to savings of energy costs by the reduction of rebolier duties. Endothermic reactions are not suitable for the RD-technology because of vapor condensation. Although endothermic reactions require more reboiler duty and therefore exhibits no large energy savings, there are no restrictions to the application of RD.

- The maximum temperature in the reaction zone is limited to the boiling point of the reaction mixture, so that the danger of hot spot formation on the catalyst is reduced significantly. A simple and reliable temperature control can be achieved.

- Product selectivities can be improved due to a fast removal of reactants or products from the reaction zone. By this, the probability of consecutive reactions, which may occur in the sequential operation mode, is lowered.

- If the reaction zone in the RD column is placed above the feed point, poisoning of the catalyst can be avoided. This leads to longer catalyst lifetime compared to conventional systems.

However applying RD-technology in industrial scale, three constraints has to be fulfilled:

- The use of RD technology is only possible, if the temperature window of the vapor-liquid equilibrium is equivalent to the reaction temperature. By changing the column operation pressure, this temperature window can be altered. However, the thermal stability of the catalyst can limit the upper operation temperature of the distillation column.

- Because of the necessity of wet catalyst pellets the chemical reaction has to take place entirely in the liquid phase.

- As it is very expensive to change the catalyst in a structured catalytic packing catalysts with a long lifetime are strongly required.

2.3.3 Effect of Operating Conditions on Performance of Reactive Distillation

Each chemical reaction has a reaction equilibrium. The chemical composition at equilibrium is such that the Gibbs free energy is minimum for a given temperature. There are some chemical reactions catalyzed by a solid catalyst for which, at a reasonable temperature, the fluid mixture at chemical reaction equilibrium still contains substantial concentrations of the unconverted reactants. Even if a high concentration of one or more of the reactants is present, the reaction may still not completely consume the stoichiometrically limiting reactant. Such reactions are generally described as equilibrium-limited reactions. For such chemical reactions, the

conversion of the limiting reactant can be substantially increased by continuous removal of the products from the reacting mixture.

Some chemical reactions have significant heats of reaction (ΔH_f) that may be exothermic or endothermic. In an adiabatic reactor, this leads to a marked change in the temperature of the reaction mixture as the reaction progresses. This large temperature change will unfavorably shift the chemical equilibrium, lower the conversion, and potentially reduce selectivity. It may also detrimentally affect catalyst stability. For such chemical reactions in a conventional process, good design may mandate splitting the reactor up into several stages with interstage cooling for exothermic reaction or interstage heating for endothermic reactions. An alternative may involve providing heat-transfer area inside the reactor. In either case, the capital cost of the equilibrium goes up.

In a reactive distillation column, the heat of reaction does not affect the temperature and, hence, the reaction equilibrium. At any point near the catalyst, the heat of reaction causes additional mass transfer (vaporization or condensation) between the vapor and liquid phases, over and above and the mass transfer occurring for distillation alone (that is, without the reaction). The temperature of the phase where the reaction occurs will be the bubble (or dew) point temperature at its composition; it will be uniform and constant across the cross-section of the column. So, heat-transfer equilibrium to remove or supply the heat of reaction is obviated. In the case of an exothermic reaction, the heat of reaction is utilized directly for the distillation. Those chemical reaction systems, that exhibit either unfavorable reaction equilibrium and significant heat of reaction can benefit the most from reactive distillation technology.

Reactive distillation is especially applicable to a certain class of reactions that employ solid catalysts. The important points that characterize such chemical/catalyst systems are the activity of the catalyst at distillation conditions and the relative volatility of the reactants and products. Proper balance between these two characteristic makes some chemical systems excellent candidates for use of the technique. A chemical/catalyst system in which the preferred temperature range of the

catalyst either matches or substantially overlaps that for the distillation is an excellent candidate for reactive distillation.

The operating pressure must also be suitable. The range of pressure for distillation is selected to provide efficient separation of the unconverted reactants and the final products, based on a number of considerations. The available condenser coolant temperature generally sets the minimum possible column pressure, while the maximum column pressure is set by the available reboiler heating-medium temperature. Within the range, the pressure should be selected so as to optimize the process economics from both capital and operating cost standpoint. A higher column operating pressure generally reduces the relative volatility of the key components, which in turn increases the reflux ratio or number of theoretical stages required for a fixed degree of separation. At a fixed diameter, the vessel wall thickness increases with increasing pressure. On the other hand, at a fixed mass loading, higher column pressure decreases the column diameter because the vapor volumetric load decreases.

The pressure of the column and the operating temperature are related by the vapor/liquid equilibrium (VLE) of the chemical system. Other considerations may include the potential for degradation or polymerization of the chemical components at the operating temperature in the column.

2.4 Aspen Plus

Aspen Plus is a component of the Aspen Engineering Suite. It is an integrated set of products designed specifically to promote best engineering practices and to optimize and automate the entire innovation and engineering workflow process throughout the plat and across the enterprise. Automatically integrate process models with engineering knowledge databases, investment analyses, production optimization and numerous other business processes. Aspen Plus contains data, properties, unit operation models, built-in defaults, reports and other features.It capabilities developed for specific industrial applications, such as petroleum simulation.

Aspen Plus is easy to use, powerful, flexible, process engineering tool for the design and steady-state simulation and optimization of process plants. Process simulation with Aspen Plus can predict the behavior of a process using basic engineering relationships such as mass and energy balances, phase and chemical equilibrium, and reaction kinetic. Given reliable thermodynamic data, realistic operating conditions and the rigorous Aspen Plus equipment models, actual plant behavior can be simulated. Aspen Plus can help design better plants and increase profitability in existing plants.

2.4.1 Features of Aspen Plus

- Utilizes the latest software and engineering technology to maximize engineering productivity through its Microsoft Windows graphical interface and its interactive client-server simulation architecture.

- Contains the engineering power needed to accurately model the wide scope of real-world applications, ranging from petroleum refining to non-ideal chemical systems to processes containing electrolytes and solids.

- Supports scalable workflow based upon complexity of the model, from a simple, single user, process unit flowsheet to a large, multi-engineer developed multi-engineer maintained, plant-wide flowsheet.

- Contains multiple solution techniques, including sequential modular, equation-oriented or a mixture of both, allows as quick as possible solution times regardless of the application.

2.4.2 Benefits of Aspen Plus

- Proven track record of providing substantial economic benefits throughout the manufacturing life cycle of a process, from R&D through engineering and into production.

- Allows users to leverage and combine the power of sequential modular and equation-oriented techniques in a single product, potentially reducing computation times by an order of magnitude while at the same increasing the functionality and suability of the process model.

- Compete effectively in an exacting environment, to remain competitive in today's process industries it is necessary to do more, often with smaller staffs and more complex process.

CHAPTER 3

LITERATURE REVIEWS

Reactive distillation is a process where chemical reaction and multistage distillation are carried out simultaneously. It especially suits chemical reactions whose conversion is limited by chemical equilibrium. By continuous separation of products from reactants while the reaction is in progress, the reaction can proceed to a much higher level of conversion than otherwise possible. Another the most important benefit of reactive distillation is a reduction of capital investment. This is because the chemical reaction and distillation are carried out in the same vassel, one process step is eliminated, along with the associated pumps, piping and instrumentation. (De Garma *et al*., 1992).

The application of the reactive distillation is quite attractive especially for production of fuel ethers such as methyl tertiary butyl ether (MTBE), tertiary amyl methyl ether (TAME) or ethyl tertiary butyl ether (ETBE), and for esterification or hydration reaction because their formations are affected by chemical equilibrium (Thiel *et al*., 1997 and Sundmach and Hoffman, 1993). The following reviews summarize the development of reactive distillation for methyl acetate production, chemical heat pump and production of oxygenates such as MTBE and ETBE. Details are given as follows.

3.1 Application of Reactive Distillation for Methyl Acetate Production

The first simple reactive distillation was developed in 1921 for the production of methyl acetate. Due to obstacle especially understanding of interaction between reaction and distillation, it took 60 years to reach the commercial Eastman Kodak process.

Nowadays, methyl acetate formation in a reactive distillation column is often used to study basic phenomena of the reactive distillation (Bessling *et al.*, 1998). In conventional methyl acetate processes, liquid methanol is reacted with liquid acetic acid in the presence of an acidic catalyst to form methyl acetate and water. The conventional processes for the manufacture of methyl acetate have to deal with the problem of refining the methyl acetate. Unreacted acetic acid can be separated easily from methyl acetate and methanol by a distillation step. A tougher problem is the purification of methyl acetate in the presence of the minimum boiling mixtures (azeotropes) of methyl acetate with water (5 wt% water, boiling point = 329.1 K) and methyl acetate with methanol (18 wt% methanol, boiling point = 326.9 K) given that the methyl acetate boiling point (330 K) is very close to that of the azeotropes.

Conventional refining schemes use vacuum columns to change the boiling points and composition of the azeotropes or use extractive agents to remove water and methanol by an extractive distillation. This, of course, requires additional distillation columns and reactive streams from distillation modeling and laboratory experiments. It was shown that the countercurrent flow of acetic acid and methyl acetate with its azeotropes can be used to purify methyl acetate.

In the conceptual basic of the countercurrent reactive distillation column, the reaction occurs in the middle section in a series of countercurrent flashing stages. Above this section, water is extracted with acetic acid and methyl acetate are separated above the acetic acid feed, in the rectification section. In the lowest column section, methanol is stripped from by-product water. Thus, refined methyl acetate is the overhead product of the reactor column while water is the bottom product.

To make the concept practical, a suitable catalyst is needed. For example, much higher concentrations of phosphoric acid are required compared to the sulfuric acid. An acetic resin such as Amberlite 200 requires complex reaction and flashing state mechanical designs. Other catalysts are simply too expensive unless a catalyst recovery system is provided (Agrada *et al.*, 1990).

The reactive distillation was implemented for other reactions between carboxylic acid and alcohol. The esterification of palmatic acid with isobutyl alcohol was studied by Goto *et al.* (1991). They found that the use of a solid ion-exchange resin as a catalyst has some advantages over a homogeneous catalyst, sulfuric acid (Goto *et al*., 1992). Other esterifications have been studied, such as the esterification of benzyl alcohol with acetic acid on Amberlyst-15 and the esterification of acetic acid with butyl alcohol to produce butyl acetate by using a sulfuric acid as a catalyst (Ventmadhavan *et al*., 1999).

3.2 Application of Reactive Distillation for Chemical Heat Pump Cycle

An interesting proposal for a heat pump cycle has attracted considerable attention. This chemical heat pump upgrades low-level thermal energy by the use of a reversible organic reaction (Cacciola *et al*., 1987). The conceptual base of the chemical reaction heat pump system is to carry out an endothermic reaction at low temperature and an exothermic reaction at high temperature. Among many chemical heat pump systems proposed to date, one promising reaction is the 2-propanol/acetone/hydrogen system. This system can raise the temperature from about 363 K to 473 K. The basic reaction system consists of the dehydrogenation of 2-propanol in the liquid phase and the hydrogenation of acetone in the vapor phase. The dehydrogenation of 2-propanol at low temperature yields acetone and hydrogen.

The dehydrogenation in the vapor phase is strongly limited by an equilibrium. On the other hand, in the liquid phase, the produced acetone is a strong inhibitor due to its large adsorption on the catalyst (Ito *et al*., 1991), and thus dehydrogenation of 2-propanol cannot proceed. It is thermodynamic limitation because the endothermic reaction is favored at high temperature while the exothermic reaction at low temperature.

To solve these two problems, Gastauer and prevost (1993) proposed a particular design for the vapor phase dehydrogenation reactor, very similar to that of the liquid phase reactor. In their proposal, the 2-propanol vapor from a vaporizer passes through a catalyst bed and enters a distillation column after reaction.

Condensed liquid 2-propanol from a separator returns to the vaporizer. All facilities include only one column. Thus, heat and mechanical energy can be saved.

Gaspillo *et al*. (1998) proposed a simple design by using a reactive distillation column. Since acetone (b.p. 602.3 K) has lower boiling point than 2-propanol (b.p. 628.4 K), acetone can be rapidly vaporized from the reaction field to avoid strong inhibition in the liquid phase dehydrogenation. The hydrogen produced remains in a gas phase throughout the operation. The use of reactive distillation, which is a pioneering idea for this chemical heat pump, can facilitate complete conversion of the dehydrogenation by overcoming two problems, that is, the limitation of equilibrium in the vapor phase and strong inhibition in the liquid phase.

Chung *et al.,* (1997) proposed an optimal design of the chemical reaction heat pump system employing the reactive distillation process through modeling and simulation by using mathematics modeling and numerical simulation. A set of 2-propanaol dehydrogenation and acetone hydrogenation reactions was used as heat transfer media. The results of simulation showed that the chemical reaction heat pump system embedded with a reactive distillation process had the better performance compared to the previous ones using a conventional distillation, because shifting the reaction equilibrium and enhancing the separation performance could be obtained simultaneously by adopting a reactive distillation process to the system. Moreover, it revealed the effect of the obtained condition such as the height of catalyst bed, the catalyst weight per stage, the total stage number and the optimal values of the reflux ratio on the system efficiency.

3.3 Application of Reactive Distillation for Octane Enhancing Ether Production

Reactive distillation is increasingly realized as a process for liquid phase synthesis of octane-enhancing ether. Methyl tertiary butyl ether (MTBE), the most widely used octane booster for reformulated gasoline, is produced in liquid phase over sulfuric acid resins (e.g., Amberlyst-15) at temperatures in the range of 323-343 K, pressure between 1.0 and 1.5 MPa, and methanol/isobutene (MeOH/IB) molar ratio higher than 1:1. Di-isobutenes (2,4,4 trimethyl-1-and-2-pentenes), *tert*-butyl alcohol,

and dimethyl ether are the main side products, the reaction is exothermic (ΔH = -37 kJ/mol), and, therefore, careful control of temperature is required in order to avoid local overheating and release of sulfonic group and sulfuric acid from the catalyst, causing a loss of activity and giving rise to corrosion problems. The MeOH/IB molar ratios above stoichiometry was employed in order to ensure complete conversion of the isobutene (Collignon *et al*., 1999).

The use of alternative catalysts for MTBE synthesis was reviewed by Hutchings *et al*. (1992). In recent years, many catalyst resins, such as zirconium phosphates (Cheng *et al*., 1992), sulfated zirconia (Quiroga *et al*., 1997) and heteropoly acids either unsupported (Matouq *et al*., 1994) or supported on silica (Shikata *et al*.,1997) were investigated. Hydrogen zeolite, steam dealuminated zeolite, and triflic acid-loaded zeolite were considered as well (Mao *et al*., 1990).

Several acidic zeolites, including H-ZSM-5 (Chu and Kuhl., 1987), large-and small-pore H-Mordenites, H-Omega, US-Y, H-Beta, and SAPD-5 were evaluated as catalysts for the vapor phase synthesis of MTBE (Collignon *et al*., 1999). It was found that zeolite H-Beta and acid Amberlyst-15 had similar activities, and were more active than other zeolites. However, the zeolite catalyst produces less by-products, this is due to the shape-selectivity of these zeolite structures, and is more thermally stable than the resin based catalysts (Mao *et al*., 1990).

Recently, there is a pending legislation of the use of methyl *tert*-butyl ether (MTBE) in a number of states in the US due to its tendency to pollute underground water. Ethyl *tert*-butyl ether (ETBE) can be a potential alternative as it has been found to outperform MTBE. ETBE has lower bRvp (4 psi) than MTBE (8-10 psi), which allows ETBE to be used successfully in obtaining gasoline with less bRvp than 7.8 psi as required in some hot places during summer (Cunill *et al*., 1993). From the environmental viewpoint, ETBE is derived from ethanol (EtOH) which can be obtained from renewable resources like biomass. It is expected that 5% of fuel used in transportation in France should be produced from renewable sources by 2005 (Poitrate, 1999).

Generally, ETBE can be produced by an exothermic reversible reaction between EtOH and isobutene (IB) on an acid catalyst, such as the acidic ion-exchange resin, Amberlyst-15. The reaction is equilibrium limited at high temperature (about 353 K) and very slow at low temperatures (below 333 K). The main side reaction is the dimerization of isobutene to form di-isobutene (DIB), but this reaction can be restricted by maintaining the ethanol concentration above 4 mol% to ensure that the catalyst surface is essentially covered with ethanol. A secondary side reaction occurs between isobutene and water - the hydration of isobutene to form tertiary butyl alcohol. This reaction can be essentially eliminated by preventing water from entering the system (Sneeby *et al*., 1997). Further, the supply of IB, which is mostly derived from non-renewale crude oil, may become limited, and for this reason alternative routes for the synthesis of ETBE are currently being explored (Rihko *et al.,* 1966). It was proposed that an alternative route was the synthesis from EtOH and *tert*-butyl alcohol (TBA) which is a major byproduct of propylene oxide production from IB and propylene in the ARCO process (Norris and Rigby, 1932).

There are two routes to produce ETBE from TBA; namely direct and indirect methods. In the indirect method, TBA is dehydrated in the first reactor to be IB, which is subsequently reacted with EtOH to produce ETBE in a second reactor. In the direct method, which is the reaction route of our interest, ETBE is produced directly from TBA and EtOH in one reactor. It is favorable not only because it shortens the process itself, but also because it would reduce demand to the purity of EtOH as the reaction produces water. As a result, the content of water in EtOH becomes unimportant (Yin *et al*., 1995) and the synthesis ETBE from TBA and EtOH at a concentration as low as that obtain from the fermentation of biomass, which EtOH concentration obtains to be maximum 2.67 mol % in aqueous solution, was report by Roukas *et al*., 1995.

Various catalysts were investigated such as Amberlyst-15 (Quitain *et al*., 1999a), Amberlyst 35, ZSM-5 and a supported flouorocarbonsulfonic acid polymer catalyst (Tau and Davis, 1989), heteropoly acid (Yin *et al*., 1995) and cation exchange resins S-54 and D-72 (Yang *et al*., 2000). A zeolitic catalyst was more attractive than resin-based catalysts in terms of higher thermal stability and no acid fume emission

(Audshoorn *et al.*, 1999). However the major side reaction of this system is the dehaydration of TBA to IB (Yin *et al.*, 1995). It was shown recently that beta zeolite provided superior selectivity compared to the commercial Amberlyst-15 (Assabumrungrat *et al*., 2002).

However, there are a limited number of works focusing on the direct synthesis of ETBE from EtOH and TBA in reactive distillation column. Matouq *et al.*, 1996 revealed that a reactive distillation column was a good choice to separated ETBE from an aqueous solution and a homogeneous catalyst. Other catalysts ($NaHSO_4$, H_2SO_4 and Amberlyst 15) failed to synthesize ETBE because the dehydration of TBA was dominant. The acid strength for these catalysts may be too strong to produce ETBE, while $KHSO_4$ has a moderate acid strength.

Quitain and Goto (1997) proposed reactive distillation which was employed to continuously synthesize ETBE from bioethanol (2.5 mol% ethanol in aqueous solution) and TBA catalyzed by Amberlyst 15 in the pallet form. At standard operating conditions, ETBE at about 60 mol% could be obtained in the distillate and almost pure water in the residue. Further extraction of the distillate obtained at standard operating conditions using the residue and the bioethanol resulted in ETBE concentration as high as 87 and 84 mol%, respectively.

In addition, a pervaporation and reactive distillation hybrid process was proposed by Yang and Goto, (1997) to improve the performance. The batch reactive distillations using Amberlyst 15 as a catalyst with and without pervaporation unit were compared. The use of pervaporation helped remove water from the residue and a higher fraction of ETBE could be obtained as a top product.

Luo and coworkers (1997) suggested a different approach. They proposed two alternative process layouts for the processing of the top product from the distillation column located after the reactor. In the first layout, the reactor effluent containing 10wt% EtOH was fed to a distillation column and the top product was processed with the pervaporation unit equipped with 30wt% cellulose acetate butyrate (CAB) and 70wt% cellulose acetate propionate (CAP) membranes. The permeate containing

99.34wt% EtOH was recycled to the reactor. The retentate was recycled to the feed position of the distillation column. In the second layout, the effluent from the reactor with 30wt% EtOH was mixed with the top product and then processed in the pervaporation unit. The EtOH-rich permeate of the pervaporation unit was recycled to the reactor, and the retentate was injected into the feed position of the distillation column. Based on the first layout, it was found that the EtOH recovery of 99.34wt%.

Quitain *et al*. (1999a) used Amberlyst 15 as a catalyst in a reactive distillation column with continuous operation. The conversion of TBA and the selectivity of ETBE were 99.9 and 35.9%, respectively. The distillate was further purified by a solvent extraction with the residual, resulting in the product with 95mol% ETBE. Later, they proposed a process for synthesizing ETBE in industrial-scale production by using Aspen Plus simulation (Quitain *et al*., 1999b).

The algorithm of the reactive distillation process by Aspen Plus has been described in more details by Venkataraman *et al.,* (1990). In addition to its application was used for the simulation of butylacetate synthesis via catalytic distiiation (Smejkal, 1998 and Hanika *et al.,*1999), 2 – Methylpropylacetae synthesis in a system of equilibrium reactor and reactive distillation column (Smejkal *et al.,* 2001), liquid – liquid equilibria of ternary 2M1B-2M2B-H_2O and quaternary 2M1B-2M2B-2M1BOH-H_2O mixture (Aiouache and Goto, 2001) and both the speedup and Aspen Plus model were compared against experimental results for the production of MTBE (Abufares and Douglas, 1995). It was noted that the simulation has also been performed, good agreement between experiment and the simulation results being achieved.

This study was aimed to use beta zeolite, which was found in our previous work that it showed superior performance compared to Amberlyst 15, for the direct synthesis of ETBE from TBA and EtOH in reactive distillation (Assabumrungrat *et al*., 2002). The best catalyst was selected from those with three Si/Al ratios and the reaction rate expressions were determined. Reactive distillation was carried out to investigate the performance at a standard condition. Finally, various operating parameters were simulated by using Aspen Plus program.

CHAPTER 4

EXPERIMENTAL

4.1 Catalyst and Supporting Material Preparation

4.1.1 Preparation of Beta Zeolite Powder

The synthesis of beta zeolite was carried out hydrothermally from the gels containing $K_2O : 2Na_2O : 12.5(TEA)_2O : 0.5Al_2O_3 : xSiO_2 : 700H_2O : yHCl$. The value of x was varied from 30 to 80 and that of y from 0 to 30. Table 4.1 shows the chemicals and their suppliers.

Table 4.1 The chemical and their suppliers

Chemical	Concentration	Supplier
Tetraethylammonium hydroxide	40% w/w	Fluka
Cataloid(a source of SiO_2)	SiO_2 30 % w/w	Aldrich
Sodium aluminate	Al/NaOH about 0.77	Wako
Sodium hydroxide	Analytical grade	Merck
Potassium chloride	Analytical grade	Ajak Chemical
Sodium chloride	Analytical grade	Merck

Table 4.2 Amount of reagents used for the preparation of beta zeolite.

Items	Weight x 10^{-3} (kg)
Tetraethylammonium hydroxide	6.2
Cataloid for Si/Al = 50	6.7
Potassium chloride	0.5
Sodium hydroxide	0.5
Sodium aluminate	0.7
NaCl	0.4

Table 4.2 also provides the amount of reagents used to prepare beta zeolite with Si/Al ratio of 55.

4.1.1.1 Gel Preparation

Tetraethylammonium hydroxide was mixed with sodium hydroxide and stirred until it became a homogeneous solution. The mixed solution was added with sodium aluminate (Al/NaOH about 0.77), potassium chloride and sodium chloride. Then it was stirred to obtain a clear solution at the room temperature. Cataloid was added dropwisely to the mixed solution. A vigorous stirrer was applied for one hour to obtain a gel.

4.1.1.2 Crystallization

The obtained gel was stirred thoroughly before transferring it to a stainless-steel autoclave. The gel was heated in the autoclave from the room temperature to 408 K in 1 hour. under the nitrogen pressure of 3 kg/cm^2 (gauge) and maintained at this temperature for 40 hours. Then, the autoclave was immersed in cold water to start a crystallization process. The obtained solid material was centrifuged at 2,500 rpm for 15 minutes and the recovered solid was washed and dried in an oven at 383 K overnight.

4.1.1.3 First Calcination

The dry solid was calcined in air stream at 813 K for 3.5 hours by heating it from the room temperature to 813 K in 1 hour. This step was to burn off the organic template and leave the cavities and channels in the crystals. Then, the calcined crystals were cooled to the room temperature in a desiccator. After this step, the crystals formed were called Na-beta zeolite.

4.1.1.4 Ammonium Ion-Exchange

The ion-exchange step was carried out by mixing the calcined crystals with 2 M NH_4NO_3 (ratio of catalyst and solution is 1g:30 cm^3) and heated on a stirring hot plate at 353 K for 1 hour. The mixture was cooled down to room temperature. Then, the ion-exchanged crystals were washed twice with de-ionized water by using a centrifugal separator. After that, the ion-exchanged crystals were dried at 383 K for at least 180 minutes in the oven. The dried crystals (NH_4- beta zeolite) were obtained.

4.1.1.5 Second Calcination

The removable species, i.e. NH_3 and NO_X were decomposed by thermal treatment of the ion-exchanged crystals in a furnace by heating them from the room temperature to 773 K in 1 hour in air stream and maintained at this temperature for 2 hours. After this step, the obtained crystals were H-beta zeolite which was used for kinetic study.

4.1.2 Preparation of Supported Beta Zeolite

Supported beta zeolite was used in kinetic study. The catalyst was made by coating the catalyst powder on a cordierite monolith obtained from N-COR Ltd., Nagoya, JAPAN. The procedures are as follows:

4.1.2.1 Preparation of Monolith Sample

The monolith test samples were prepared by cutting the cordierite monolith (400 cell/in^2) into small cube supports (0.5x0.5x0.5 cm^3).

4.1.2.2 Surface Treatment

The monolith supports were weighted and soaked in 2.5 wt% acetic acid solution for 2 minutes. After that, they were washed by distilled water several times to remove residual acid solution and then dried in an oven at 383 K until the weight became constant.

4.1.2.3 Preparation of Slurry for Wash Coat

Beta zeolite powder was added into 2.5 wt % acetic acid solution to give 30-50% wt/volume beta zeolite wash coat and the obtained slurry was stirred for 5-10 minutes.

4.1.2.4 Monolith Coating Procedure

The monolith supports were dipped into the prepared washcoat for 15 minutes and followed by drying at 383 K overnight in the oven. The supports were repeatedly dipped in the washcoat 2-3 times and calcined at 773 K for 3.5 hours in air atmosphere.

4.1.3 Characterization of the Catalysts

4.1.3.1 X-Ray Diffraction Patterns

X-Ray Diffraction (XRD) patterns of the catalysts were performed with SIEMENS XRD D5000, accurately measured in the 4-44° 2θ angular region, at petrochemical Engineering Laboratory, Chulalongkorn University.

4.1.3.2 X-Ray Fluorescence Spectrometer (XRF)

The silicon and aluminum content of the prepared catalyst was analyzed by X-Ray Fluorescence spectrometer (XRF) at the Scientific and Technological Research Equipment Center, Chulalongkorn University (STREC).

4.1.3.3 Specific Surface Area Measurement (BET)

Specific surface area *(S_{BET})* of the catalysts was calculated by using a Brunauer-Emmett-Teller (BET) single point method on a basis of nitrogen uptake measured at a liquid-nitrogen boiling point temperature.

4.1.3.3.1 BET apparatus

An experimental apparatus of the single point BET surface area measurement consisted of two feed lines of helium and nitrogen. The flow rates of both gases were adjusted by means of fine-metering valves connected with a thermal conductivity detector. A sample cell is made from pyrex glass. The schematic diagram of the experimental apparatus is shown in Figure 4.1 and an operating condition of the thermal conductivity detector within a gas chromatograph (GOW-MAC) is illustrated in Table 4.3.

Table 4.3 Operating condition of a thermal conductivity detector within a gas chromatograph (GOW-MAC) for measurement of the specific surface area

Model	GOW-MAC
Detector type	TCD
Helium flow rate	30 ml/min
Detector temperature	303°C
Detector current	80 mA

4.1.3.3.2 BET procedure

A gas mixture of helium and nitrogen flowed through a system at the nitrogen relative pressure of 0.3. A catalyst sample was placed in the sample cell, ca. 0.2 g, which was heated up to 433 K and then held at this temperature for 2 hours in order to remove the remaining water on catalyst surface. Subsequently, it was cooled down to room temperature and measured the specific surface area containing.

1. Adsorption step: The catalyst sample set in the sample cell was dipped into the liquid nitrogen. Nitrogen gas flowing through the system was adsorbed on catalyst surface of the sample until equilibrium was reached.

2. Desorption step: The sample cell containing the nitrogen-adsorbed catalyst sample was rapidly dipped into water at room temperature. The adsorbed nitrogen gas was desorbed from the catalyst surface. This step was absolutely completed when an apparent signal on a recorder was back in a position of a base line drift.

3. Calibration step: 1 ml of nitrogen gas at atmospheric pressure was injected through an injection port. An obtained integral area of this gas was used as a reference area for calibration. A calculation method will be explained separately in Appendix C.

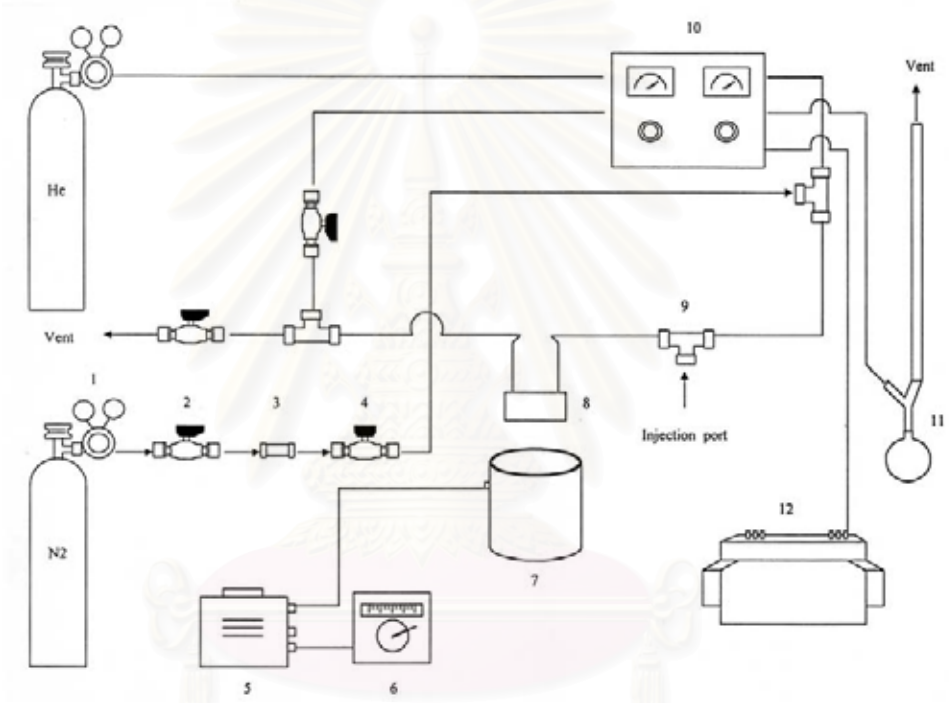

1. Pressure Regulator 2. On-off Valve 3. Gas Filter
4. Needle Valve 5. Voltage Transformer 6. Temperature Controller
7. Heater 8. Sample Cell 9. Three-way
10. Thermal Conductivity Detector 11. Bubble Flow Meter 12. Recorder

Figure 4.1 Schematic diagram of the single point BET specific surface area measurement

4.1.3.4 Acidity Measurement by NH_3-TPD

The acid properties were observed by Temperature programmed desorption (TPD) equipment at PTT Research and Technology Institue.

4.1.3.4.1 NH_3-TPD procedure

1. 0.2 g of a catalyst sample was placed in a quartz tubular reactor. Under helium atmosphere at a flow rate of 10 ml/min, the catalyst sample was heated up to 737 K at a heating rate of 283 K/min and held for 1 hour at this temperature in order to eliminate the adsorbed water. Then, the system was cooled down to 353 K.

2. At 353 K, the adsorption step was carried out in 10%v/v NH_3/He at a flow rate 20 ml/min for 40 minutes. After the adsorption step, the catalyst sample was swept in helium until a base line of the TCD signal was constant.

3. The desorption step was performed under a helium flow of 30 ml/min from room temperature to 943 K at a heating rate of 278 K/min.

4.1.3.5 Scanning Electron Microscope (SEM)

The distribution of beta zeolite with Si/Al ratio 55 on surface area of monolith were observed by JEOL Scanning Electron Microscope (SEM) at the Scientific and Technological Research Equipment Center, Chulalongkorn University (STREC)

4.2 Catalyst Selection

4.2.1. Semi Batch Reactor Apparatus

The reactor consisted of a three-necked flask of $0.25x10^{-3}$ m^3 capacity fitted with a condenser in the central opening, a liquid sampling syring and a thermometer. The reaction temperature was controlled by a water bath. The mixture was magnetically stirred at the maximum speed of 660 rpm in all the runs for the reason that the external mass transfer resistance was negligible.

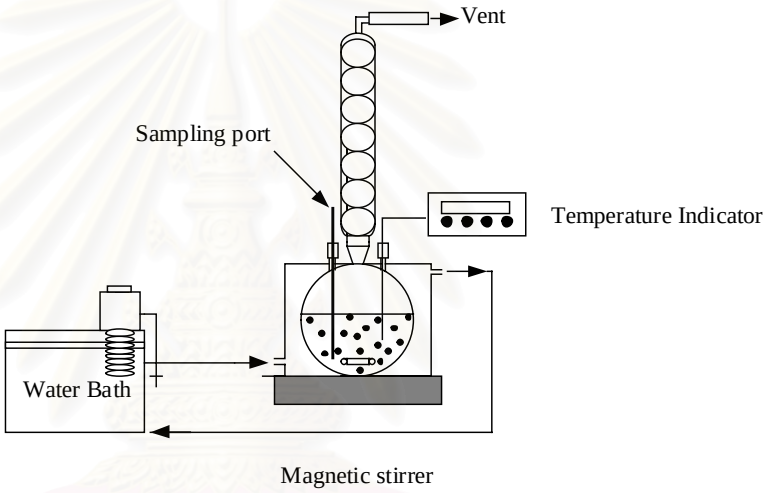

Figure 4.2 Schematic diagram of the catalyst selection experimental set-up

4.2.2 Experimental Procedure

1. 1 mol of TBA and 1 mol of EtOH was measured and placed into the reactor.
2. The solution was heated to the desired reaction temperature (333 K) and stirred at about 660 rpm
3. 10 g of the catalyst was added to start the reaction
4. Approximate $1x10^{-6}$ m^3 samples were taken every hour for analysis.

4.2.3 Analysis

The analysis was carried out in a gas chromatograph. The operating condition of a gas chromatography was shown in Table (4.4). Separation was achieved for all components.

Table 4.4 Operating condition of gas chromatography

	Condition
Detector	TCD
Packed column	Gaskuropack 54
Column length	2.5 m
Mesh size of packing	60/80
Helium flow rate	30 cm^3/min
Column temperature	443 K
Injector temperature	453 K
Detector temperature	453 K

4.3 Kinetics Study

4.3.1 Kinetic Study Apparatus

Kinetic study of the supported beta zeolite was carried out in a specially-designed reactor as shown in Figure 4.3. A jacketed reactor was maintained at a constant temperature by circulating hot water in the jacket around the chamber. A heater with a temperature controller was used to control a water temperature while a condenser was equipped with the system to condense all vapors in the reaction chamber. The reactor had four connectors for connecting a condenser, a rotating shaft, sampling port and thermocouple. A frame of four catalyst baskets (as illustrated in Figure 4.4) was equipped with a rotating shaft, which was driven by a motor via an inverter controller. The cylindrical baskets were made of stainless steel tubes with a wall made of stainless steel mesh.

4.3.2 Experimental Procedure

1. 2 moles of EtOH and TBA were placed into the reactor.
2. The supported catalyst of 15 g beta zeolite was packed in four catalyst baskets.
3. The frame was held above the liquid level by upper hooks as shown in Figure4.4 (a) to prevent the reaction occurring.
4. Four-bladed disk turbine was used to stir the liquid mixture during heating up period.
5. After temperature was maintained at a desired value (T = 323-343 K), the reaction was started by inverting the direction of agitation so that the frame of basket dropped into the liquid mixture. The lower hooks were securely connected with slots on the disk turbine and the frame was rotated with slip as shown in Figure 4.4 (b).
6. Approximate $1x10^{-6}$ m^3 samples were taken every hour for analysis.

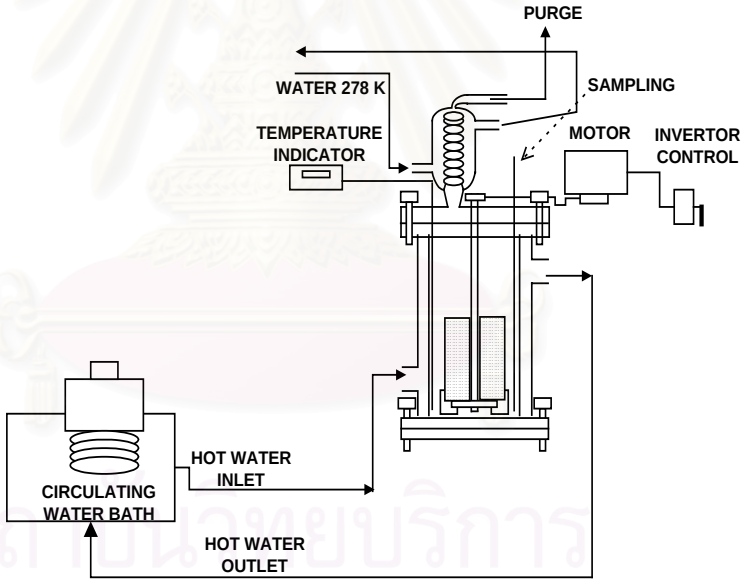

Figure 4.3 Schematic diagram of the kinetic studied experimental set-up

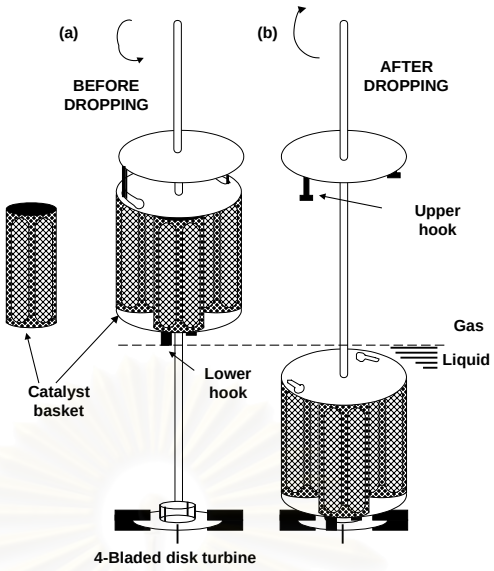

Figure 4.4 Detail of catalyst basket assembly

(a) Before dropping

(b) After dropping

4.4 Reactive Distillation Study

4.4.1 Reactive Distillation Apparatus

Figure 4.5 shows a schematic diagram of the set-up a four-neck round bottom flask with a mantle heater served as a reboiler. The heat duty at the reboiler was controlled by a slidac. A vacuum-insulated column (inside diameter = 3.5 cm, height = 60 cm) was connected to the central opening of the flask, about 45 g of catalyst was placed inside the column (height = 18 cm) to allow simultaneous reaction and separation of products. Stainless steel mesh saddles (48 mesh, 3 mm diameter, 6 mm height) were used as packing materials for rectifying and stripping sections of the column (height = 21 and 21 cm, respectively). Thermocouples were connected to measure the temperature profiles inside the column. Circulating water at a temperature of 288 K served as a coolant for the condenser located at the top. A gas meter was connected to measure the amount of IB gas escaping from the condenser. The reflux ratio was controlled by the solenoid valve with a multitimer.

4.4.2 Reactive distillation procedure

A mixture of TBA, EtOH, H_2O was placed inside the bottom flask and heated up to boiling point. When distillate appeared at the top, feed mixture of TBA, EtOH and H_2O at room temperature was introduced to the lower part of the reaction section by using a peristaltic pump. At the same time, liquid from the reboiler was withdrawn by another peristaltic pump. Then, continuous operation was started. The liquid level in the reboiler was maintained by adjusting the tip of the withdrawing pipe connected to the pump. The experiment was conducted for about 7 hours. After every hour, the ditillate and the residue were collected, weighed and analyzed.

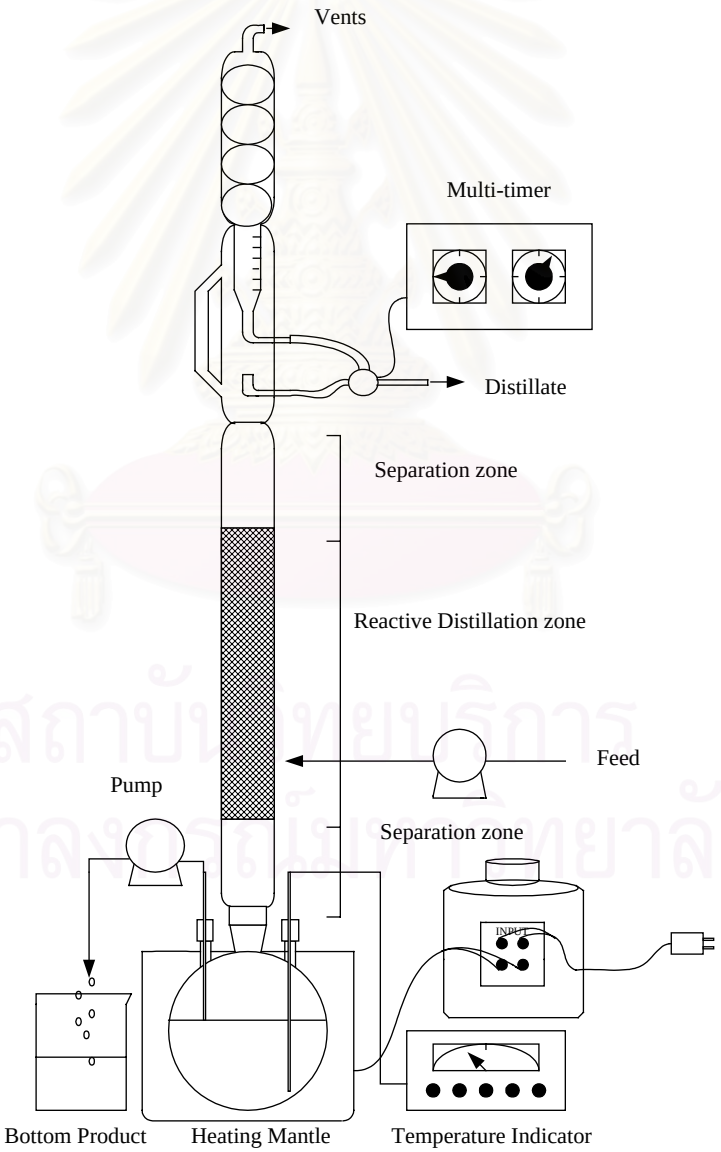

Figure 4.5 Schematic diagram of reactive distillation system

CHAPTER 5

RESULTS AND DISCUSSION

5.1 Catalyst Characterization

Various techniques were employed to characterize beta zeolite catalysts, i.e. X-Ray Diffraction (XRD), X-Ray Fluorescence spectrometer (XRF), BET surface area, Temperature Programmed Desorption (TPD) and Scanning Electron Microscope (SEM). The following sections provide the details of the characterization results.

5.1.1 X-Ray Diffraction (XRD)

XRD was a technique-employed here to confirm structure of the synthesized beta zeolite. The XRD pattern of the synthesized catalyst (shown in Figure5.1) was compared with that of a standard beta zeolite (shown in Figure 5.2) obtained from Ramesh *et at.*, 1992. The values of 2θ ranged between 4^o and 44^o. The same diffraction pattern was observed and, hence, it was concluded that the synthesized catalyst was a beta zeolite.

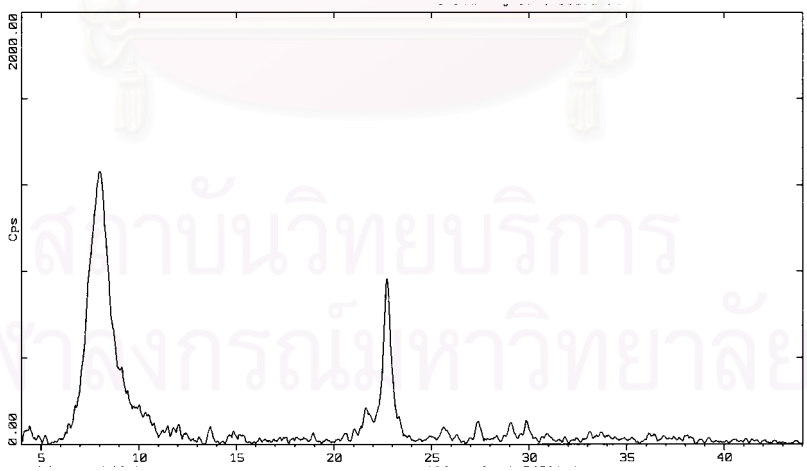

Figure 5.1 X-ray diffraction pattern of synthesized catalyst (Si/Al=36)

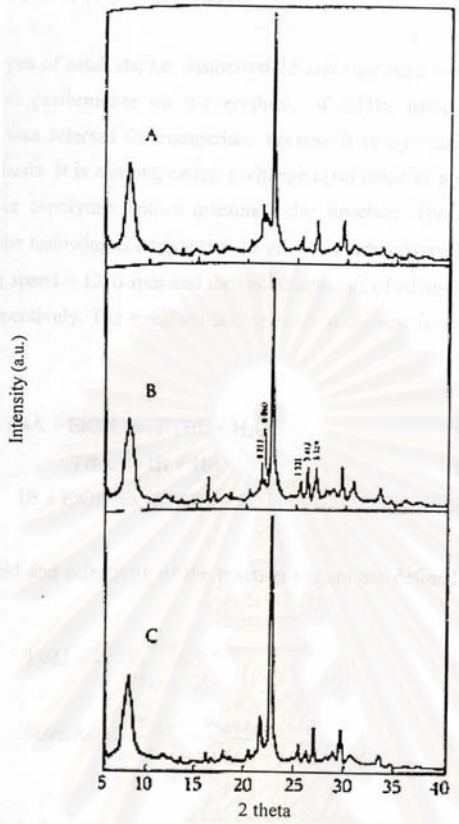

Figure 5.2 X-ray diffraction pattern of standard beta zeolite (Ramesh et al., 1992)
Si/Al : A = 19.7, B = 12.2, C = 10.5

5.1.2 X-Ray Fluorescence Spectrometer (XRF)

The quantitative analysis of compositions of silicon (Si) and aluminum (Al) in the beta zeolite were carried out using the XRF spectrometer. Table 5.1 compared the values of the Si/Al ratio observed from XRF and those from the specification of for the commercial beta zeolite with Si/Al of 13.5 and 55 and from the calculation based on the initial ratio of raw materials for the synthesized beta zeolite with the ratio of 50. The observed Si/Al ratio of the commercial zeolite agreed very well with their specifications; however, significant deviation was noticed for the synthesized zeolite. The observed value of 36 will be used as the Si/Al ratio of the synthesized zeolite for the rest of the studies.

Table 5.1 Si/Al content in beta zeolites

Si/Al ratio of beta zeolite	Si/Al ratio observed
13.5	13.45
50	36.23
55	54.88

5.1.3 BET Surface Area

Table 5.2 showed BET surface area of the beta zeolite. It was observed that the surface areas were almost the same regardless of the different values of the Si/Al ratio.

Table 5.2 BET surface areas of beta zeolite

Beta zeolite	BET surface area (m^2/g of beta zeolite)
H-Beta (Si/Al = 13.5)	635
H-Beta (Si/Al = 36)	618
H-Beta (Si/Al = 55)	628

5.1.4 Temperature Programmed Desorption (TPD)

TPD was a useful technique to characterize the acid properties of the catalyst. The results shown in Figure 5.3 revealed that the higher the Si/Al ratio, the higher the acid strength the lower the acidity. The former property was observed from the peak at desorption temperature while the latter was observed from the area of peak. Since the number of oxygen atoms, which were related to polar anionic framework and interaction with highly polar molecules such as water and acidic OH groups depend on the number of aluminium in zeolite framework. It should be noted that the beta zeolite with Si/Al ratio of 55 had the highest acid strength but the lowest acidity.

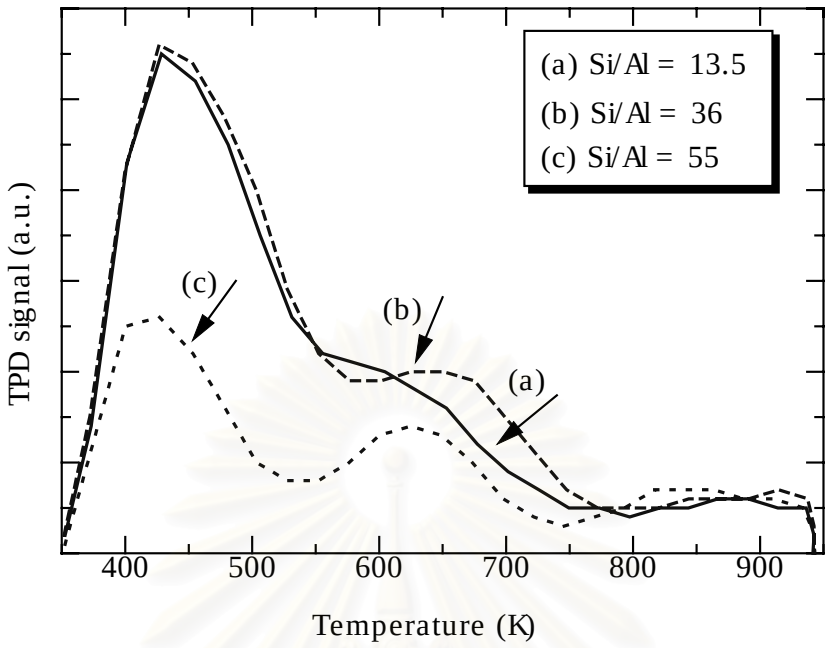

Figure 5.3 TCD profile of beta zeolite with different Si/Al ratio

5.1.5 Scanning Electron Microscope (SEM)

Figure 5.4 showed distribution of beta zeolite on surface area of monolith. It was plugging of beta zeolite in some of cell open area, it might be caused by decreasing the efficiency of supported catalysts.

Figure 5.4 SEM photographs of supported beta zeolite

5.2 Catalyst Selection

Three Si/Al ratios of beta zeolite were investigated in a semi-batch reactor. A reactant mixture containing 1 mole of TBA and 1 mol of EtOH was poured into the reactor as described in section 4.2.2. After the solution was magnetically stirred and heated up to 333 K, the reaction was started by adding 10 g of the beta zeolite into the reactor.

The reaction-taking place in the reactor can be summarized as follows:

$$EtOH_{(l)} + TBA_{(l)} \Longleftrightarrow ETBE_{(l)} + H_2O_{(l)} \quad (5.1)$$

$$TBA_{(l)} \Longleftrightarrow IB_{(g)} + H_2O_{(l)} \quad (5.2)$$

$$EtOH_{(l)} + IB_{(g)} \Longleftrightarrow ETBE_{(l)} \quad (5.3)$$

Here, %conversion of TBA and %selectivity of ETBE were defined as follows:

$$\%\text{Conversion of TBA} = (M_{TBA(0)} - M_{TBA}) / M_{TBA(0)} \quad (5.4)$$

$$\%\text{Selectivity of ETBE} = (M_{ETBE} - M_{ETBE(0)}) / (M_{TBA(0)} - M_{TBA}) \quad (5.5)$$

The reverse reaction in Eq.(5.2) and the reaction in Eq.(5.3) were neglected since the operating pressure in this study was at atmospheric pressure and, consequently, only small amount of IB can be dissolved in the liquid. The forward reaction of Eq.(5.2) was considered as a major side reaction of this reaction system.

Figure 5.5 showed the effect of Si/Al ratio on the reaction conversion and selectivity of ETBE. It was observed that both of them were not significantly affected by the change of the Si/Al ratio. Although it was reported by Matouq *et al.,* 1994 and Collinon *et al.,* 1999 that the acid properties and the surface area of catalyst were main parameters on the performance of this system, the range of the acid properties in this study seems not to influence the catalyst performance. In the following studies, the beta zeolite with the Si/Al ratio of 55 was selected, as it was commercial available and presented in a ready-to-use form unlike that with the ratio of 13.5 which was carried out a second calcination to convert the NH_3 for to the H form.

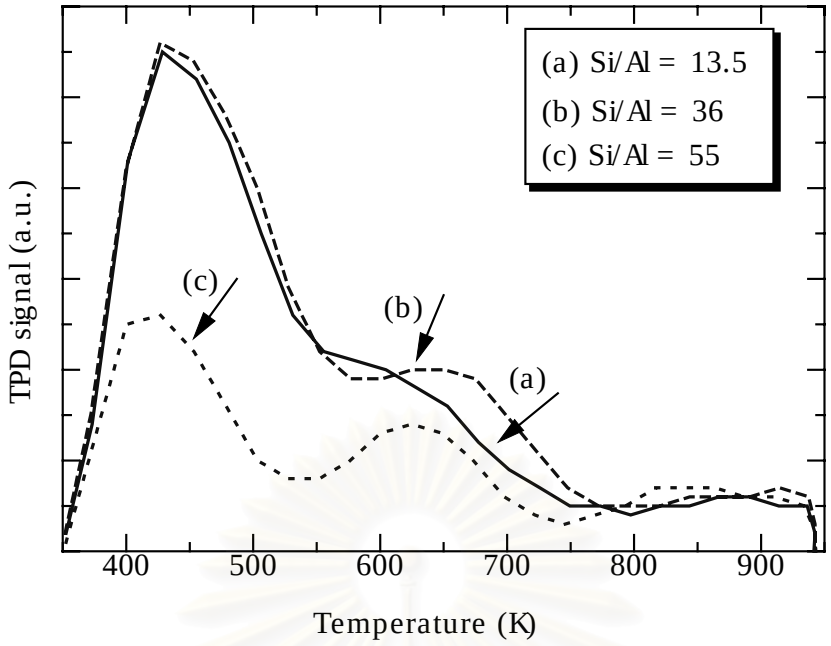

Figure 5.5 The performance of beta zeolite with difference Si/Al ratio

5.3 Kinetic Study

5.3.1 Development of Mathematical Models

Mathematical descriptions were developed for both concentration-based and activity-based models. Since the solubility of IB in the liquid mixture was low under atmospheric condition. The reaction of IB with EtOH or H_2O was negligible. As a result, the rate laws of the reactions (5.1) and (5.2) can be expressed in terms of concentrations as

$$r_1 = k_{1c} \frac{(c_{TBA} c_{EtOH} - c_{ETBE} c_{H_2O} / K_{1c})}{1 + K_{Wc} c_{H_2O}} \tag{5.6}$$

$$r_2 = k_{2c} \frac{c_{TBA}}{1 + K_{Wc} c_{H_2O}} \tag{5.7}$$

and in terms of activities as

$$r_1 = k_{1a} \frac{(a_{TBA} a_{EtOH} - a_{ETBE} a_{H_2O} / K_{1a})}{1 + K_{Wa} a_{H_2O}} \tag{5.8}$$

$$r_2 = k_{2a} \frac{a_{TBA}}{1 + K_{Wa} a_{H_2O}} \tag{5.9}$$

where k_{jc} and k_{ja} were reaction rate constants of reaction j (j = 1, 2) in the concentration-based and activity-based models, respectively. c_i and a_i were concentration and activity of species i, respectively. K_1 was the equilibrium constant. K_{Wc} and K_{Wa} were water inhibition parameters from the concentration-based and activity-based models, respectively. The expression of K_{1a} and K_{1c} were assumed to be the same and can be expressed as follows (Quitain *et al*.,1999)

$$K_{1a} = K_{1c} = \exp(-1.23 + 944/T) \tag{5.10}$$

By performing a material balance for a semi-batch reactor, the following expressions are obtained.

$$-\frac{dm_{TBA}}{dt} = \frac{dm_{H_2O}}{dt} = W(r_1 + r_2) \tag{5.11}$$

$$-\frac{dm_{EtOH}}{dt} = \frac{dm_{ETBE}}{dt} = Wr_1 \tag{5.12}$$

Where m_i and W represented the number of mole of species i and the catalyst weight, respectively. It was noted that the number of moles in the liquid phase at any time was constant because IB can only slightly dissolved in the liquid phase. In addition, every one mole of TBA consumption produced one mole of water, and every one mole of EtOH consumption produced one mole of ETBE. The activity can be calculated from the following relation.

$$a_i = \gamma_i x_i \tag{5.13}$$

where x_i was mole fraction of species i in the liquid mixture and γ_i was the activity coefficient. The activity coefficients can be calculated using the UNIFAC method as in Appendix B. (Gmehling *et al*., 1982).

5.3.2 Kinetic Parameter Determination

A set of experiments was carried out at three temperature levels to investigate the kinetic parameters. Figures 5.6, 5.7 and 5.8 showed typical results of mole changes with time at T = 323, 333 and 343 K, respectively. The initial moles of each species were given in the figure captions. They can be seen that the production of ETBE becomed higher with the increase of temperature as expected in the Arrhenius' equation. However, the selectivity decreased because the dehydration of TBA to IB and water in Eq.(5.2) proceeds at relatively faster rate than the main reaction at higher temperature.

A curve fitting method was employed to find the kinetic parameters, k_{1c}, k_{2c} and K_{wc} for the concentration-based model and k_{1a}, k_{2a} and K_{wa} for the activity-based model at each temperature. Initial guess values of the parameters k_{1c}, k_{2c}, k_{1a} and k_{2a} were obtained by using an initial rate method (Fogler, 1992). The dashed lines in the figures represent the simulation results from the concentration-based model while the solid lines represent those from the activity-based model using the corresponding parameters. It was found that within the ranges of study, both models agreed well with the experimental results . However, it should be noted that the activity-based model was more suitable for a liquid phase reaction since its performance usually deviates from ideality. Nevertheless, the concentration-based parameters were also included in this study to meet the requirement of the Aspen Plus simulator.

Figure 5.9 showed the Arrhenius plot of the reaction rate constants while Figure 5.10 showed the Van't Hoff plot of the adsorption parameters.

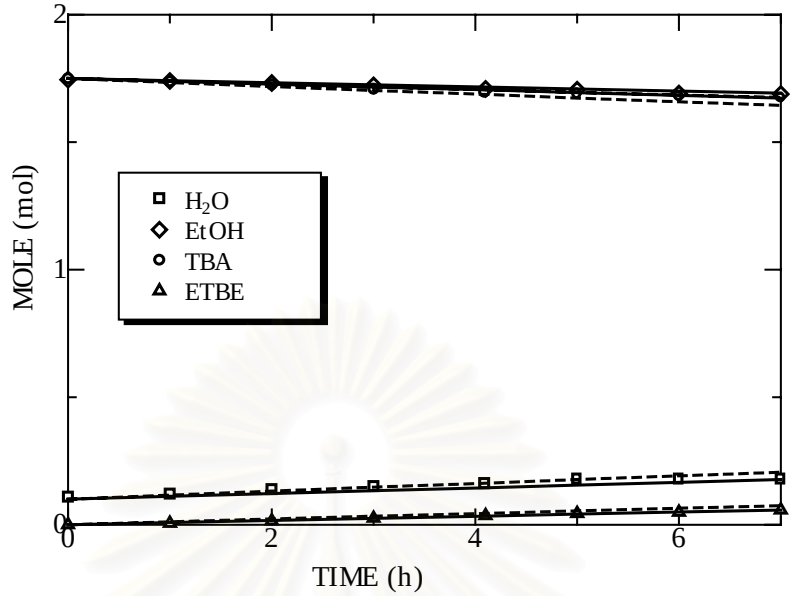

Figure 5.6 Mole change with time (Catalyst = beta zeolite with Si/Al=55, catalyst weight = 15 g, $M_{TBA,0}$ = 1.75 mol, $M_{EtOH,0}$ = 1.75 mol, $M_{H2O,0}$ = 0.10 mol, $M_{ETBE,0}$ = 0 mol and T = 323 K)

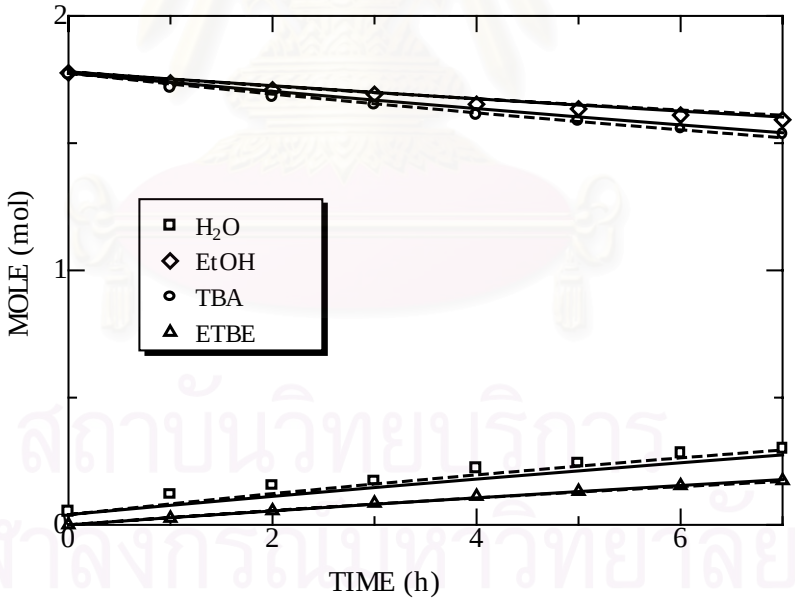

Figure 5.7 Mole change with time (Catalyst = beta zeolite with Si/Al=55, catalyst weight = 15 g, $M_{TBA,0}$ = 1.78 mol, $M_{EtOH,0}$ = 1.78 mol, $M_{H2O,0}$ = 0.04 mol, $M_{ETBE,0}$ = 0 mol and T = 333 K)

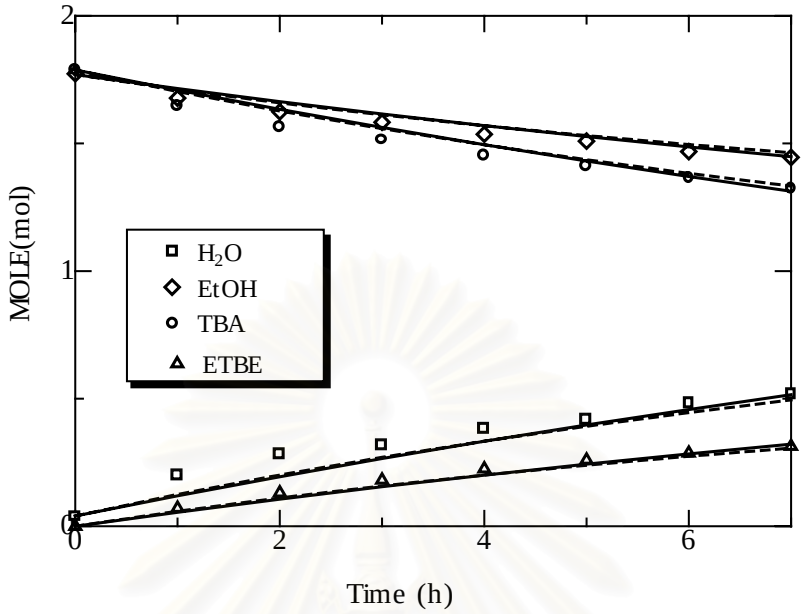

Figure 5.8 Mole change with time (Catalyst = beta zeolite with Si/Al=55, catalyst weight = 15 g, $M_{TBA,0}$ = 1.79 mol, $M_{EtOH,0}$ = 1.77 mol, $M_{H2O,0}$ = 0.04 mol, $M_{ETBE,0}$ = 0 mol and T = 343 K)

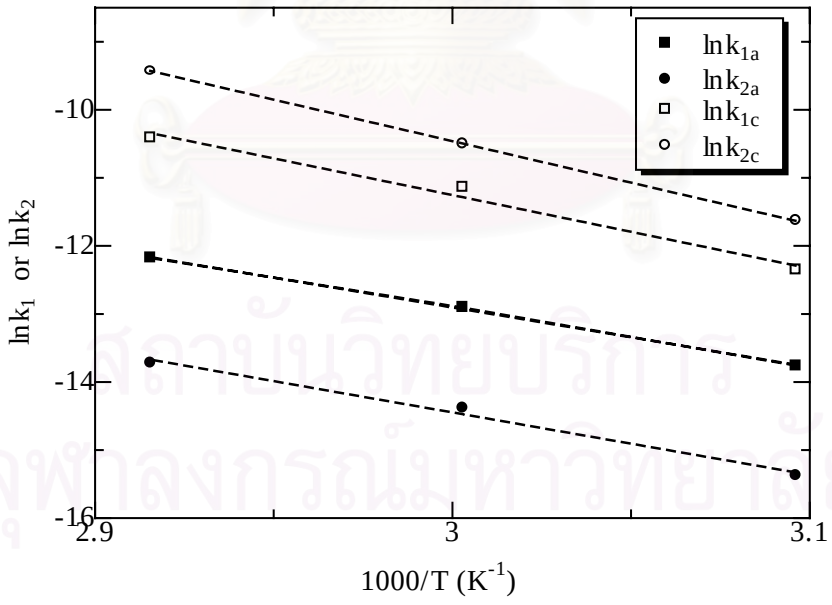

Figure 5.9 Arrhenius plot

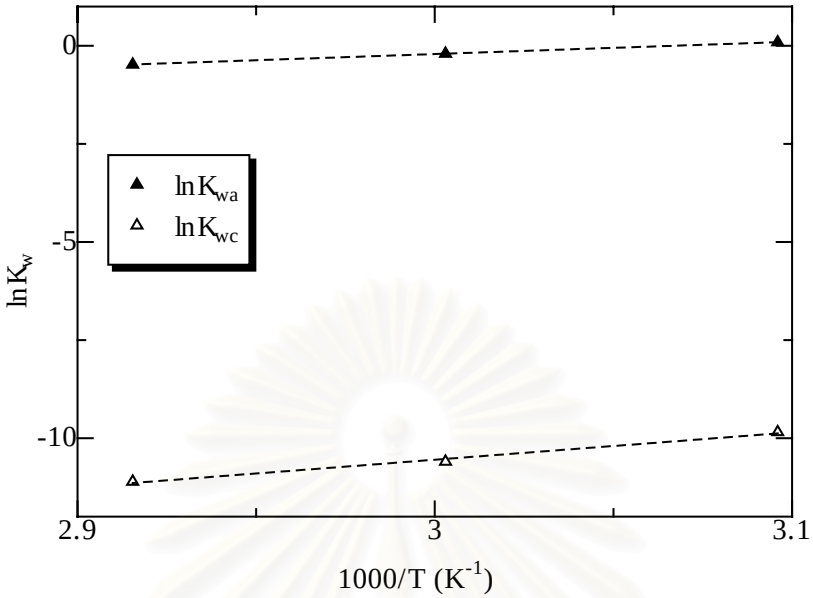

Figure 5.10 Van't Hoff plot

The following equations were determined from the plots.

Concentration-based model:

$$k_{1c} = \exp(21.10 - 10785 / T) \quad (5.14)$$

$$k_{2c} = \exp(26.13 - 12199 / T) \quad (5.15)$$

$$K_{Wc} = \exp(-31.56 + 7003 / T) \quad (5.16)$$

Activity-based model:

$$k_{1a} = \exp(13.37 - 8758 / T) \quad (5.17)$$

$$k_{2a} = \exp(13.12 - 9189 / T) \quad (5.18)$$

$$K_{Wa} = \exp(-9.68 + 3156 / T) \quad (5.19)$$

The values of the activation energy of the reactions in Eq. (5.1) and Eq. (5.2) were 90 and 101 kJ/mol from the concentration-based model, respectively, and 73 and 76 kJ/mol from the activity-based model, respectively. The enthalpy of water adsorption was -58 and -26 kJ/mol from the concentration-based model and the activity-based model, respectively.

5.4 Reactive Distillation Study

5.4.1 The Performance of Reactive Distillation at Standard Condition

An experiment was carried out at the standard condition shown in Table 5.3. The mole fraction profiles for both the residue and the distillate were shown in Figure 5.11. H_2O was the main component of the bottom product whereas in the distillate contained 18.2 mol% ETBE, 32.4 mol% TBA, 19.4 mol% EtOH and 28.3 mol% H_2O.

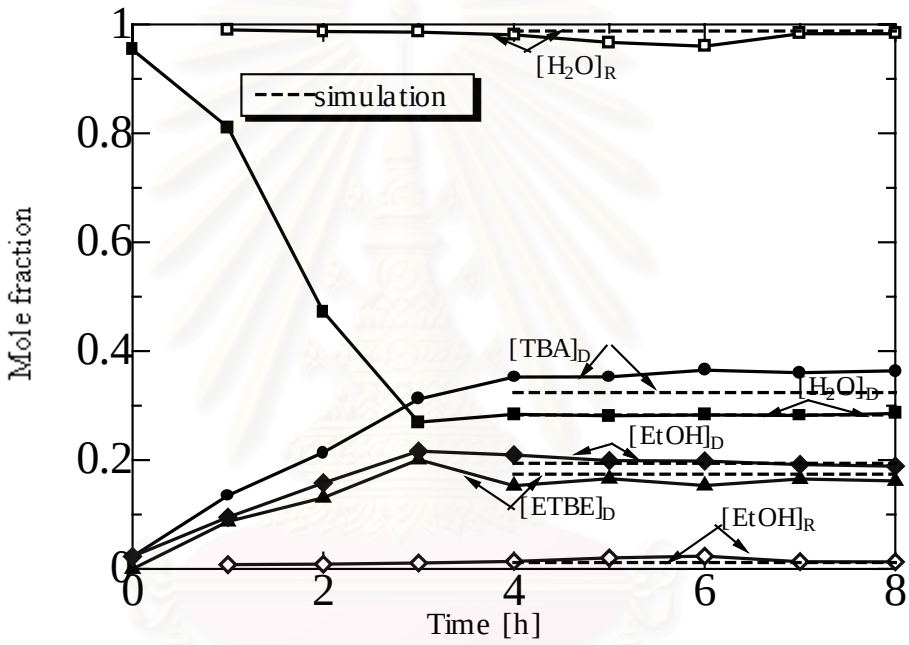

Figure 5.11 Concentration profiles of distillate and residue at standard operating condition (Feed flow rate = 0.16 mol/min, Reflux ratio = 1.5, Catalyst = 0.045 kg and Molar ratio of TBA:EtOH:H_2O = 1:1:38)

The terms conversion of TBA (X_{TBA}) and selectivity of ETBE (S_{ETBE}) were used to represent the performance of the reactive distillation and they were defined as follows:

$$X_{TBA} = \frac{\text{Molar flow rate of TBA reacted}}{\text{Feed molar flow rate of TBA}} \times 100\ \%$$

$$S_{ETBE} = \frac{\text{Molar flow rate of ETBE in the liquid distillate}}{\text{Molar flow rate of TBA reacted}} \times 100\ \%$$

The corresponding conversion and selectivity at the standard condition were 60.5% and 27.7 %, respectively.

The RADFRAC module of Aspen Plus can also be used to simulate the RD column. In the simulation, a property option set PSRK based on the predictive Soave-Redlich-Kwong equation of state was used.

Figure 5.12 showed the column configuration used in the simulation. The column consisted of 16 stages, including a partial reboiler (stage 16) and a partial condenser (stage 1). The reaction section in the middle of the column was represented by six reactive stages (stage 6-11). The reaction was assumed to take place in the liquid phase. The feed was introduced at the stage 10. The simulation input to Aspen Plus was mainly based on experimental operation conditions. However, reflux ratio defined in Aspen Plus was the reflux liquid flow *(L1)* from the condenser (stage 1) divided by the total distillate flow *(D = LD+VD), L1/D.* This definition was different from the experimental reflux ratio *(L1/LD)* because the liquid flow from the condenser was distributed into *L1* and *LD* using a multitimer.

RADFRAC simulation requires two more input parameters which can be chosen from the following four parameters; heat duty at reboiler *(Q)*, condenser temperature *(T_c)*, ratio of total distillate flow to feed *(D/F)* and ratio of vapor distillate to total distillate *(VD/D).* It should be noted that the two parameters, the temperature condenser and heat duty were chosen because it was difficult to control the values of *D/F* and *VD/D* in practical operation.

Table 5.3 also provided the column specification for Aspen Plus simulation for the experimental result at the standard condition.

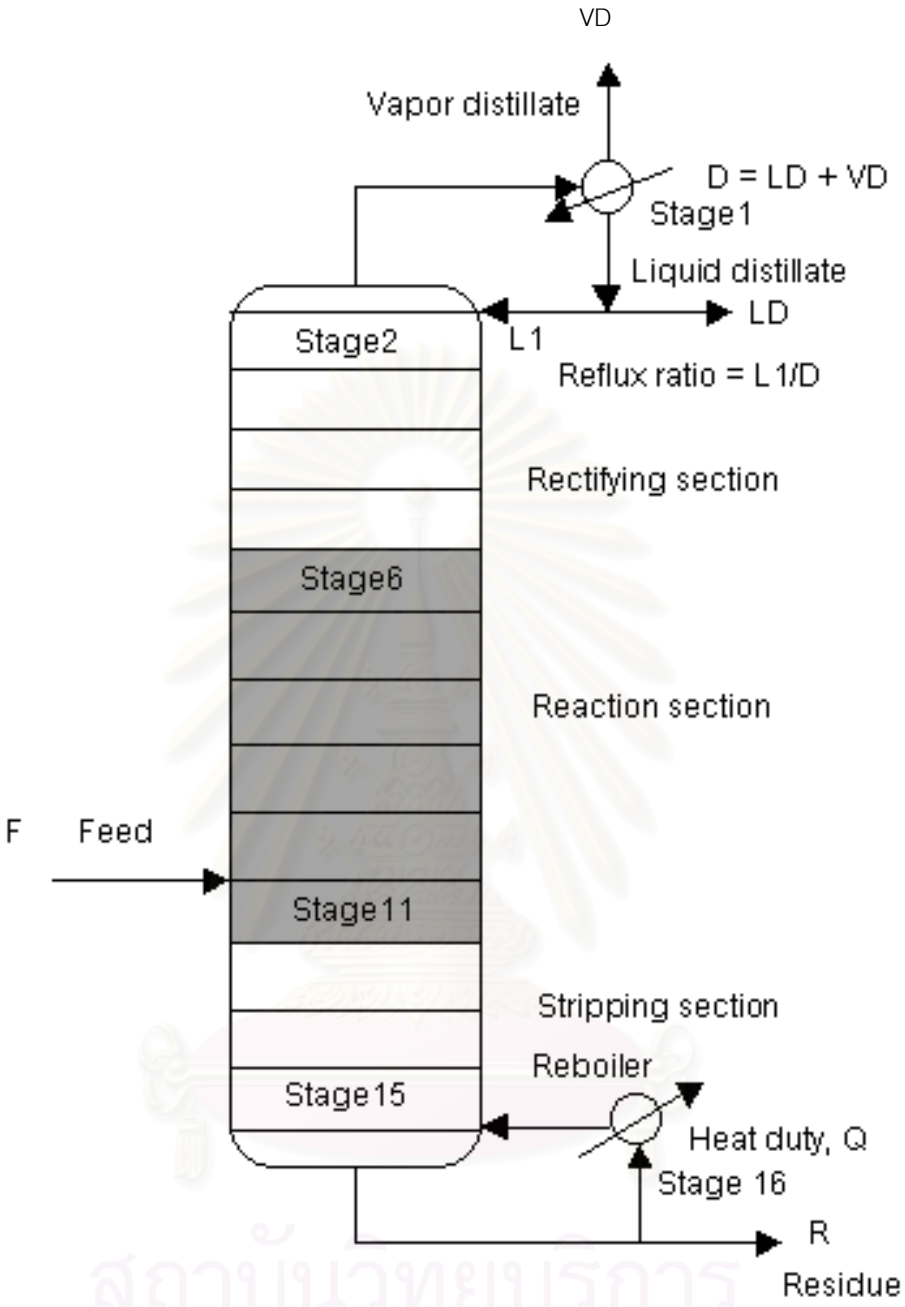

Figure 5.12 Reactive distillation column simulation input to Aspen Plus under standard conditions

Table 5.3 Reactive distillation column simulation input to Aspen Plus under standard conditions

Feed Condition		Column Specification	
Temperature [K]	298	Rectification stages	5
Flow rate x 10^3 [mol/sec]	2.71	Reaction stages	6
Molar ratio (TBA:EtOH:H_2O)	1:1:38	Stripping stages	5
Composition [% mole]		Total stages	16
EtOH	2.5	Catalyst weight per stage [kg]	0.065
TBA	2.5	Pressure [kPa]	101.3
H2O	95	Reflux ratio [L_1/D]	1.5
Pressure [kPa]	101.3	Condenser temperature [K]	332
		Heat duty [W]	26.3

The dash lines in Figure 5.11 showed the simulation results from the program. It was obvious that the simulation results agree well with the experimental results.

5.4.2 Effect of Operating Parameters

Aspen Plus program was used to simulate the performance of reactive distillation in order to study the effects of various operating parameters. Here the effects of the condenser temperature, feed flow rate, reflux ratio, heat duty and molar ratio of H_2O:EtOH were investigated.

Effect of the condenser temperature

The effect of the condenser temperature was investigated by varying the T_c values between 303 and 333 K. As shown in Figure 5.13, the increasing in the condenser temperature significantly affected the selectivity of ETBE but not for the conversion. It was obvious that the increase of the condenser temperature raised the quantities of the vaporized distillate of the reactants and products, therefore decreasing the selectivity.

It should be noted that the selectivity could be improved by lowering the condenser temperature since the selectivity of 27.67% was obtained when using the condenser temperature of the experiment *Tc* = 333 K but the value as high as 43.10% could be obtained at lower condenser temperature of *Tc* = 303 K. Accordingly the latter temperature was selected for the subsequent studies.

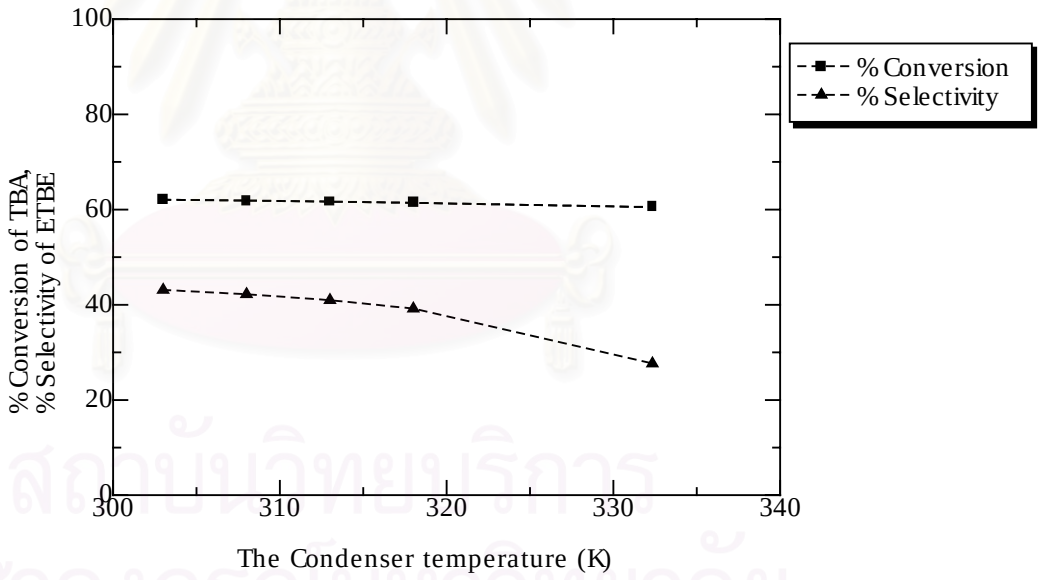

Figure 5.13 Effect of the condenser temperature on conversion of TBA and selectivity of ETBE (Catalyst = beta zeolite with Si/Al of 55, Catalyst weight = 45 g, feed flow rate = 2.7×10^{-3} mol/sec, reflux ratio = 1.5:1, heat duty = 26.3 W and molar ratio of TBA:EtOH:H_2O = 1:1:38)

Effect of feed flow rate

Figure 5.14 shown the effect of feed flow rate on the conversion of TBA and the selectivity of ETBE. The condenser temperature was fixed at 303 K and the other operating parameters were the same as the standard condition. It was observed that there was an optimum total feed molar flow rate which offered the maximum conversion and selectivity. From the optimum value, increasing feed flow rate decreased the conversion and selectivity. As the amount of catalyst, reflux ratio and heat duty were fixed, the increase in flow rate resulted in the decrease in the residence time and column temperature, thus reducing the conversion. Although the higher selectivity should be expected from the lower column temperature, the opposite trend was observed. It was probably due to there was higher amount of water in the column when increasing feed flow rate and the forward reaction 5.1, hence, was suppressed. Unlike the reaction 5.1, that of the reaction 5.2 was not occurred.

However, at the optimum feed flow rate, decreasing feed flow rate decreased the conversion and the selectivity. It was due to the reactants could be easily vaporized and present in the distillate as unconverted reactants.

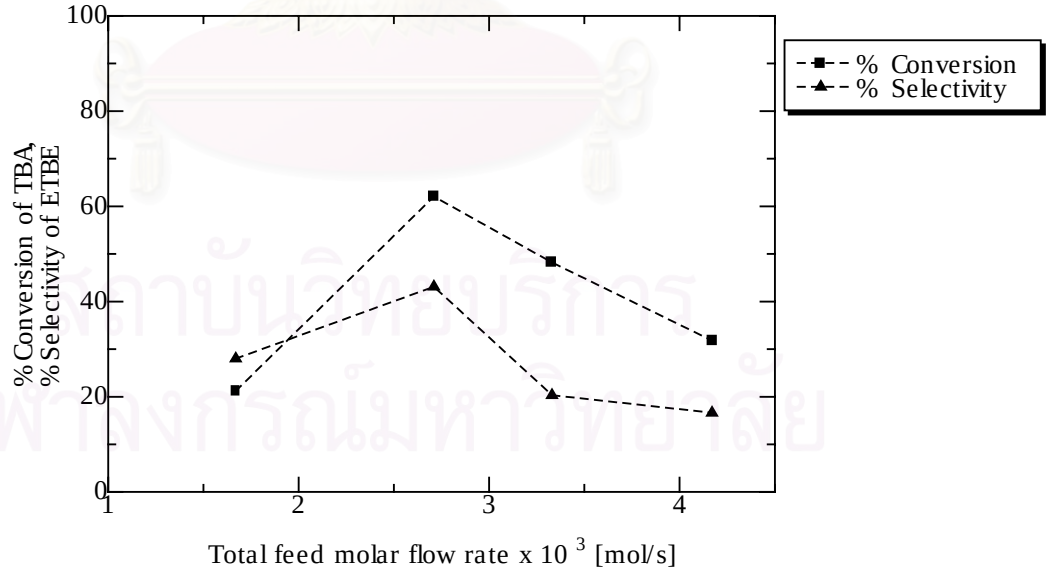

Figure 5.14 Effect of feed flow rate on conversion of TBA and selectivity of ETBE (Catalyst = beta zeolite with Si/Al of 55, Catalyst weight = 45 g, *Tc* = 303 K, reflux ratio = 1.5:1, heat duty = 26.3 W and molar ratio of TBA:EtOH:H_2O = 1:1:38)

Effect of reflux ratio

In Aspen Plus, the reflux ratio was defined as the reflux liquid flow from the condenser (stage1, L1) divided by the total distillate flow (D). Figure 5.15 showed the conversion and selectivity as a function of the reflux ratio. Increasing the reflux ratio from 0.6 to 2.0 raised the conversion but reduced the selectivity. Increasing the reflux ratio increased the residence time of the reactants. In the other words, the unconverted reactants were refluxed into the column; consequently, the conversion was increased. Because the H_2O concentration of liquid in the column was higher when increasing reflux ratio, the backward reaction of the reaction 5.1 was significant than that of the reaction 5.2, hence decreasing the selectivity. In addition, a high reflux ratio was economically unattractive as it adds to the equipment size and energy requirements.

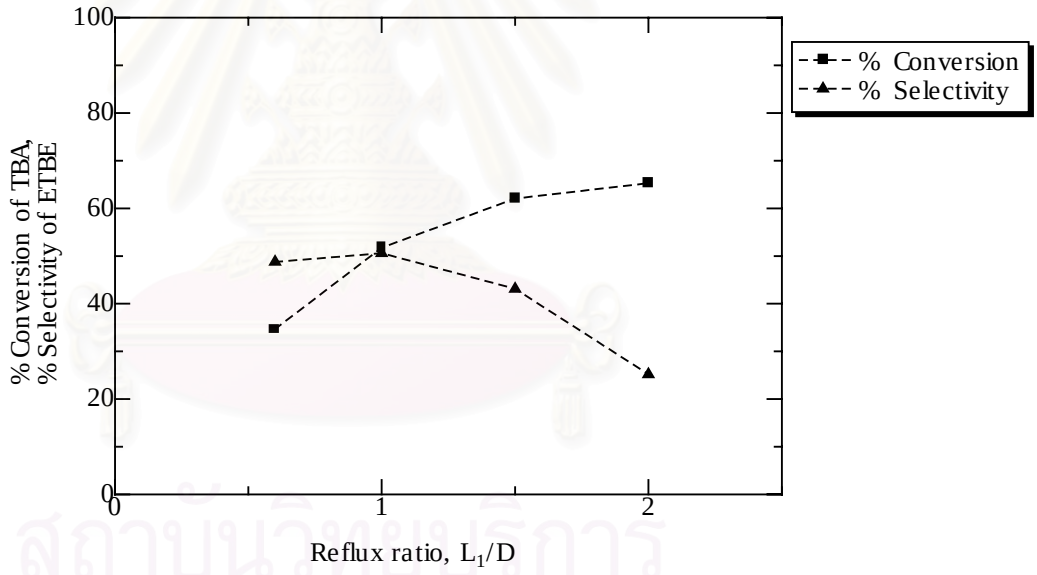

Figure 5.15 Effect of reflux ratio on conversion of TBA and selectivity of ETBE (Catalyst = beta zeolite with Si/Al of 55, Catalyst weight = 45 g, *Tc* = 303 K, feed flow rate = 2.7×10^{-3} mol/sec, heat duty = 26.3 W and molar ratio of TBA:EtOH:H_2O = 1:1:38)

Effect of heat duty

The effect of heat duty was investigated as shown in Figure 5.16. Conversion increased initially and then dropped at high value while selectivity increased with increasing heat duty. Increasing the heat duty resulted in the increase of the vapor load in the column. Due to the fixed reflux ratio and feed flow rate, the higher unconverted reactants appeared in the distillate and, consequently, the conversion decreased. However, it was noted that there was a minimum heat duty sufficient to vaporize the reactant and to keep the column temperature at high value.

The increasing selectivity at higher heat duty might be due to the desired product of distillate could be condensed at chosen *Tc*.

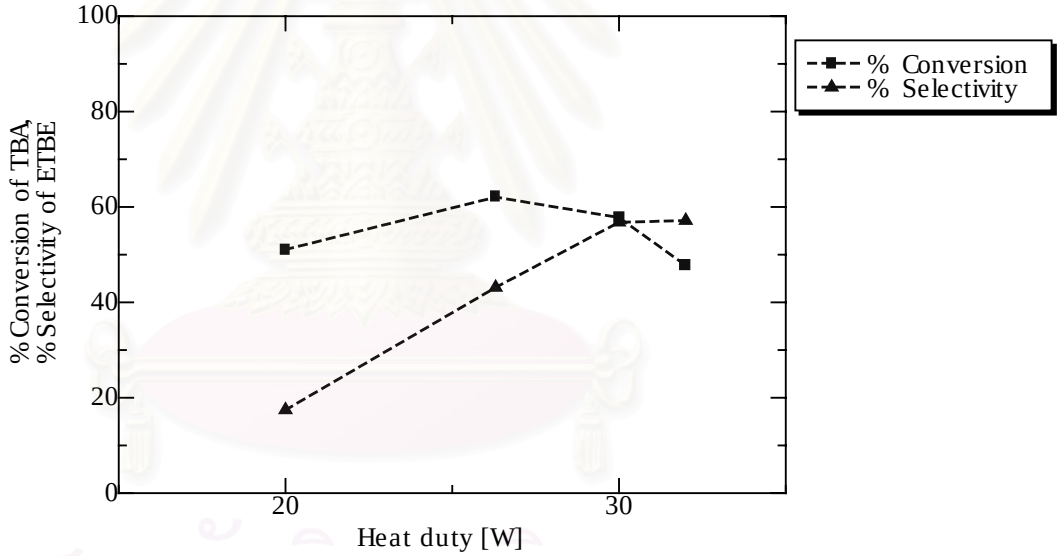

Figure 5.16 Effect of heat duty on conversion of TBA and selectivity of ETBE (Catalyst = beta zeolite with Si/Al of 55, Catalyst weight = 45 g, *Tc* = 303 K, feed flow rate = 2.7×10^{-3} mol/sec, reflux ratio = 1.5:1 and molar ratio of TBA:EtOH:H_2O = 1:1:38)

Effect of molar ratio of H_2O:EtOH

EtOH derived from fermentation usually contains the significant amount of H_2O. Figure 5.17 shows the effect of H_2O concentration in feed expressed as the molar ratio of H_2O to EtOH. Five values of 10:1, 20:1 30:1, 38:1 and 60:1 were investigated. The molar ratio of TBA:EtOH was equal to 1. It was found that the conversion increased initially and then dropped when increasing the molar ratio but the trend of selectivity was opposite. Because the reactant concentrations and reactant feed flow rate decreased with the increasing molar ratio, the former tended to decrease the rate of reaction while the latter tended to improve the reaction extent. Thus these completing effects resulted in the observed conversion results.

As shown in this figure, the improved selectivity might be because the column temperature was lowered at higher molar ratio of H_2O: EtOH. However, the opposite trend was observed. This might be similar to the case of the increasing feed flow rate.

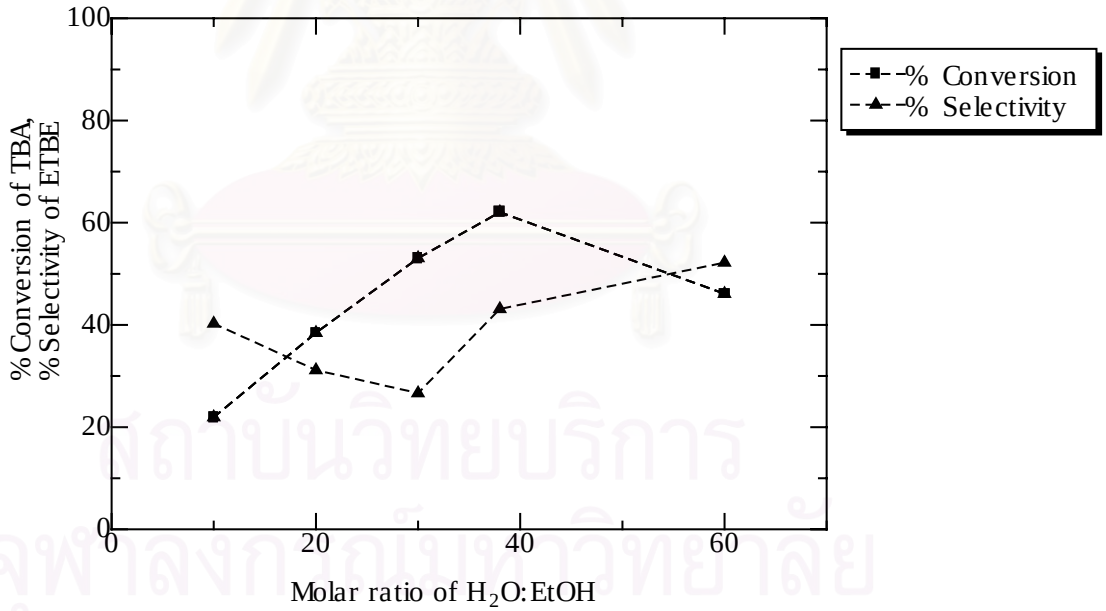

Figure 5.17 Effect of molar ratio of H_2O:EtOH on conversion of TBA and selectivity of ETBE (Catalyst = beta zeolite with Si/Al of 55, Catalyst weight = 45 g, *Tc* = 303 K, feed flow rate = 2.7×10^{-3} mol/sec, reflux ratio = 1.5:1 and heat duty = 26.3 W)

CHAPTER 6

CONCLUSIONS AND RECOMMENDATIONS

Conclusions

In this thesis, application of reactive distillation for production of ETBE from EtOH and TBA was studied.

The reactions taking place in the reactor can be summarized as follows:

$$EtOH_{(l)} + TBA_{(l)} \Longleftrightarrow ETBE_{(l)} + H_2O_{(l)} \quad (1)$$

$$TBA_{(l)} \Longleftrightarrow IB_{(g)} + H_2O_{(l)} \quad (2)$$

$$EtOH_{(l)} + IB_{(g)} \Longleftrightarrow ETBE_{(l)} \quad (3)$$

The studies were divided into 3 sections; i.e. catalyst selection, kinetic study and reactive distillation study. The results could be concluded as shown in the following sections.

1. Catalyst selection:

In a previous work, it was obvious that beta zeolite offered higher selectivity than other catalysts. In this study, three beta zeolites with different Si/Al ratio (13.5, 36 and 55) were tested in a semi-batch reactor. It was observed that both the conversion of TBA and the selectivity of ETBE were not significantly affected by the change of the Si/Al ratio. The range of the acid properties in this study seemed not to influence the catalyst performance.

2. Kinetic study

Kinetic parameters, which were an important data for the simulation of the reactive distillation column in Aspen Plus program, were determined. The following kinetic parameters based on the concentration-based model and the activity-based model were obtained:

Concentration-based model:

$$k_{1c} = \exp(21.10 - 10785 / T)$$

$$k_{2c} = \exp(26.13 - 12199 / T)$$

$$K_{Wc} = \exp(-31.56 + 7003 / T)$$

Activity-based model:

$$k_{1a} = \exp(13.37 - 8758 / T)$$

$$k_{2a} = \exp(13.12 - 9189 / T)$$

$$K_{Wa} = \exp(-9.68 + 3156 / T)$$

3. Reactive distillation study

Results under the standard condition indicated that H_2O was the main component of the bottom products whereas the component of the distillate contained 18.2 mol% ETBE, 32.4 mol% TBA, 19.4 mol% EtOH and 28.3 mol% H_2O. The conversion of TBA and the selectivity of ETBE were 60.51% and 27.67%, respectively.

The effects of various operating parameters on the reactive distillation performance were investigated by using the Aspen Plus simulator and the following conclusions could be drawn from the study:

1. Increasing the condenser temperature significantly affected the selectivity of ETBE but the conversion remained unaltered. So the improved selectivity of this system could be obtained by using *Tc*=303 K.

2. The total feed molar flow rate at 2.71×10^{-3} mol/sec was an optimum value which offered the maximum conversion and selectivity.

3. Increasing the reflux ratio raised the conversion but reduced the selectivity. This was due to it increased the residence time of the reactants and also the concentration of water in column.

4. Increasing the heat duty resulted in the increase of vapor load in the column. However, due to the fixed reflux ratio, the higher unconverted reactants appeared in the distillate and, consequently, the conversion decreased. There was a minimum heat duty sufficient to vaporize the reactant and to keep the column temperature a high value.

5. When increasing the molar ratio of H_2O:EtOH, the conversion increased initially and then dropped but the trend of selectivity was opposite.

Recommendations

From kinetics study, it was found that selectivity decreased with increasing temperature because the dehydration of TBA to IB proceed fast at the higher rate compared to the formation of ETBE. In addition, from the reactive distillation experiment at the standard condition, the rather poor performance; i.e. conversion = 60.51% and selectivity = 27.67%, were observed. Although the best performance can be obtained by changing the operating condition such as lowering the condenser temperature, the complete conversion of TBA to ETBE could not be obtained. To improve the ETBE production it is recommended as follows:

1. A pervaporation unit should be combined with the reactive distillation column to help the remove of water from the column.

2. Another reactive distillation column should be included in the process to further react IB with EtOH to form ETBE.

REFERENCES

Abufares, A.A. and P.L. Douglas; "Mathematics modeling and simulation of an MTBE catalytic distillation process using speed up and Aspen Plus," *Trans IChem*., 73 (1995).

Agrada, V.H., L.R. Partin and W.H. Heise; "High-Purity Methyl Acetate *via* Reactive Distillation," *Chem.Eng. Prog*., 86, 40-46 (1990).

Assabumrungrat S., Kiatekittipong, W., Sevitoon N., Praserthdam P. and Goto S.; "Kinetics of Liquid Phase Synthesis of Ethyl tert-Butyl Ether from tert-Butyl Alcohol and Ethanol Catalyzed by beta-Zeolite Supported on Monolith" *Int. J. of Chem. Kinetics*., 42**,** 6-10 (2002)**.**

Audshoorn, O.L., M. Janissen, W.E.J. van Kooten, J.C. Jansen, H. van Bekkum, C.M. van den Bleek and H.P.A. Calis; "A Novel Structured Catalyst Packing for Catalytic Distillation of ETBE," *Chem. Eng. Sci*., 54, 1413-1418 (1999)**.**

Bessling, B., J.M. Loning, A.Ohilgschlager, G. Schembecker and K. Sundmacher; "Investigation on the Synthesis of Methyl Acetate in a Heterogeneous Reactive Distillation Process," *Chem. Eng. Tech*., 21, 393-400 (1998).

Bisowarno, B.H. and M.O. Tade; "Dynamic Simulation of Startup in Ethyl *tert*-Butyl Ether Reactive Distillation with Input Multiplicity," *Ind. Eng. Chem. Res.*, 39, 1950-1954 (2000).

Cacciola, G., V. Anikeev, V. Recuperd, V. Kirillov and V. Parmon; "Chemical heat pump using heat of reversible catalyst reactions," *Int. J. Eng. Res.*, 11, 519-529 (1987).

Chu, P., and G.H. Kuhl; "Preparation of Methyl *tert*-Butyl Ether (MTBE) over Zeolite Catalysis," *Ind. Eng. Chem. Res.*, 26, 365-369 (1987).

Collignon, F., R. Loenders, J.A. Martens, P.A. Jacobs and G. Poncelet; "Liquid Phase Synthesis of MTBE from Methanol and Isobutene Over Acid Zeolites and Amberlyst-15," *J. of Cat.*, 182, 302-312 (1999).

Cunill, F., M. Vila, J.F. Izquierdo, M. Iborra and J. Tejero; "Effect of Water-Presence on Methyl tert-Butyl Ether and Ethyl tert-Butyl Ether Liquid Phase Syntheses," *Ind. Eng. Chem. Res*., 32, 564-569 (1993).

De Garmo, J.L., V.N. Parulekar, and V. Pinjala; "Consider Reactive Distillation," *Chem. Eng. Prog.*, 43-50 (1992).

Gaspillo, P.A.D., L,C. Abella and S. Goto; “Dehydrogenation of 2- Propanol in Reactive Distillation Column for Chemical Heat Pump,” *J. of Chem. Eng. of Japan*, 31, 440-444 (1998).

Gautauer, P. and M. Prevost; “Dehydrogenation of Isopropanol at low temperature in the vapor phase as reaction for a chemical heat pump,” *J. Chem. Eng. Japan,* 26, 580-583 (1993).

Goto, S., T. Yagawa and A. Yusoff; “A. Kinetics of the Esterification of Palmatic Acid with Isobutyl Alcohol,” *Int. J. of Chem. Kint.,* 23, 17-23 (1991).

Goto, S., M. Takeuchi and M.H. Matouq; “Kinetics of Esterification of Palmatic Acid with Isobutyl Alcohol on Ion-Exchange Resin Pellets,” *Int. J. of Chem. Kint.,* 24, 587-592 (1992).

Hanika, J., J. Kolena and Q. Smejkal; “ Butylacetate via reactive distillation-modelling and experimental,” *Chem. Eng. Sci.*, 54, 5205-5209 (1999).

Hutchings, G.J., C.P. Nicolaides and M.S. Scurrell; “Developments in the production of methyl *tert*-butyl ether,” *Catal Today,* 15, 23 (1992).

Ito, E., M. Yamashita, S. Hagiwara and Y. Saito; “A Composite Ru-Pt Catalyst for 2-Propanol Dehydrogenation Adaptable to the Chemical Heat Pump System,” *Chem. Lett.,* 351-354 (1991).

Mao, R.L.V., R. Carli, H. Ahlafi and V. Ragaini; “Synthesis of Methyl tertiary Butyl Ether (MTBE) over Triflic Acid Loaded ZSM-5 and Y Zeolites” *Cat. Lett.,* 6, 321-330 (1990).

Luo, G.S., M. Niang and P. Schaetzel; “Separation of ethyl tert-butyl ether-ethanol by combined pervaporation and distillation,” *Chem. Eng. J.*, 68**,** 139-143 (1997).

Matouq, M., and S. Goto,. “Kinetics of Liquid-Phase Synthesis of Methyl *tert*-Butyl Ether from *tert*-Butyl Alcohol and Methanol Catalyzed by Ion-Exchange Resin,” *Int. J. Chem. Kint., 2*5, 825-831 (1993).

Matouq, M., T. Tagawa and S. Goto; “Combined Process for Production of Methyl *tert*-Butyl Ether from *tert*-Butyl Alcohol and Methanol,” *J. of Chem. Eng. of Japan*, 27, 302-306 (1994).

Matouq, M., A. Quitain, K. Takahashi and S. Goto; “Reactive Distillation for Synthesizing Ethyl *tert*-Butyl Ether from Low-Grade Alcohol Catalyzed by Potassium Hydrogen Sulfate,” *Ind. Eng. Chem. Res.*, 35, 982-984 (1996).

Norris J.F. and G.W. Rigby, “The Reactivity of Atoms and Groups in Organic Compounds,” *J. Am. Chem. Soc.*, 54, 2088-2100 (1932).

Oudshoorn, O.L., M. Janissen, W.E.J. van Kooten, J.C. Jansen and H.A. van Bekkum, "Novel Structure Catalyst Packing for Catalytic Distillation of ETBE," *Chem. Eng. Sci.*, 54, 1413-1418 (1999).

Poitrate, E.; "The Potential of Liquid Biofuel in France," *Renewable Energy*, 16, 1084-1089 (1999).

Rihko, L.K. and A.O. Krause; "Etherification of FCC light gasoline with methanol," *Ind.Eng.Chem.Res*., 35, 2500-2507 (1996).

Quitain, A., H. Itoh and S. Goto; "Reactive Distillation for Synthesizing Ethyl tert-Butyl Ether from Bioethanol," *J. Chem. Eng. Japan*, 32, 280-287, (1999a).

Quitain, A., H. Itoh and S. Goto; "Industrial-Scale Simulation of Proposed Process for Synthesizing Ethyl *tert*-Butyl Ether from Bioethanol," *J. Chem. Eng. Japan*, 32, 539-543, (1999b).

Smejkal, Q.; "Simulation of reactive distillation of butyl acetate," *Ph.D. Thesis. Institute of Chemical Technology Prague* (1998).

Smejkal, Q., J. Hanika and J. Kolena; "2-Methylpropylacetace synthesis in a system of equilibrium reactor and reactive distillation column," *Chem. Eng. Sci.*, 56**,** 365-370 (2001).

Sneesby, M.G., M.O. Tade, R. Datta, and T.N. Smith; "ETBE Synthesis via Reactive Distillation. 2. Dynamic Simulation and Control Aspects," *Ind. Eng. Chem. Res.*, 36, 1870-1881 (1997).

Sneesby M.G., M.O. Tade and T.N. Smith; "Two-Point Control of a Reactive Distillation Column for Composition and Conversion," *Journal of Process Control*, 9, 19-31 (1999).

Stichlmair, J.G. and T. Frey; "Reactive Distillation Processes," *Chem. Eng. Tech.*, 22, 95–103 (1999).

Tau, L.M. and R.H. Davis; "Acid Catalyzed Formation of Ethyl tertiary Butyl Ether (ETBE)" *App. Cat*., 53, 263-271 (1989).

Tayler, R. and R. Krishna; "Review: Modelling Reactive Distillation," *Chem. Eng. Sci.*, 55, 5183-5229 (2000).

Thiel, C., K. Sundmacherd and U. Hoffmann; "Synthesis of ETBE: Residue curve maps for the heterogeneous catalyzed reactive distillation process," *Chem.Eng.J.*, 66, 181-191 (1997).

Ventmadhavan, G., Malone, M.F., and Doherty, M.F. "A Novel Distillation Policy for Batch Reactive Distillation with Application to the Production of Butyl Acetate," *Ind. Eng. Chem. Res.*, 38, 714-722 (1999).

Yang, B. and S. Goto; "Pervaporation with Reactive Distillation for the Production of Ethyl *tert*-Butyl Ether," *Sep. Sci. Tech*., 32, 971-981 (1997).

Yang, B., S. Yang and R. Yao; "Synthesis of Ethyl *tert*-Butyl Ether from *tert*-Butyl Alcohol and Ethanol on Strong Acid Cation-Exchange Resins," *Reactive and Functional Polymers*, 44, 167-175, (2000).

Yin, X., B. Yang and S. Goto, "Kinetics of Liquid-Phase Synthesis of Ethyl tert-Butyl Ether from tert-Butyl Alcohol and Ethanol Catalyzed by Ion-Exchange Resin and Heteropoly Acid," *Int. J. Chem. Kinetics*, 27, 1065-1074 (1995).

APPENDICES

APPENDIX A

CORRECTION FACTOR

From raw data of gas chromatography analysis, mole fraction of each component can be calculated by using correction factors.

$$\text{Mole (M)} = \text{Weight / Molecular weight} \qquad \text{(A.1)}$$

$$\text{Correction factor (F)} = \frac{\text{Area ratio}}{\text{Mole ratio}} = \frac{(A_i / A_{standard})}{(M_i / M_{standard})} \qquad \text{(A.2)}$$

Given Ethanol (EtOH) is the standard component (F=1), subscript i identifies species and molecular weight of EtOH, TBA, H_2O and ETBE is 46, 74, 18 and 102 respectively.

These following tables show steps of calculation for the correction factors.

No.	Weight				Mole			
	EtOH	TBA	H_2O	ETBE	EtOH	TBA	H_2O	ETBE
1	3.6060	0	0	0.4649	0.0783	0	0	0.0045
2	6.6460	6.2795	0	0	0.1443	0.0847	0	0
3	10.9514	0	0.9850	0	0.2377	0	0.0547	0
4	3.2679	5.4126	1.0734	0	0.0709	0.0730	0.0596	0
5	4.2215	5.9093	0.4657	0.2942	0.0916	0.0797	0.0259	0.0029

The obtained average correction factors of EtOH, TBA, H_2O and ETBE are 1, 0.7462, 2.1220 and 0.6008 respectively. These factors are used to calculate mole of each component in a liquid mixture as follows.

$$\text{Mole fraction } (X_i) = (\text{Mole ratio})_i / \Sigma \text{ mole ratio} \qquad \text{(A.3)}$$

$$= \{(\text{Area ratio})_i \times F_i\} / \Sigma \text{ mole ratio} \qquad \text{(A.4)}$$

$$= \frac{(A_i / A_{standard}) \times F_i}{\Sigma \text{ mole ratio}} \qquad (A.5)$$

No.	Area				Area ratio		
	EtOH	TBA	H_2O	ETBE	TBA/EtOH	H_2O/EtOH	ETBE/EtOH
1.	2120875	0	0	208628	0	0	0.0983
2.	1245799	972916	6081	0	0.7809	0.0049	0
3.	2278491	0	247287	0	0	0.1085	0
4.	339670	470384	133918	0	1.3848	0.3943	0
5.	379648	444418	50702	19533	1.1706	0.1336	0.0515

No.	Mole ratio			Correction Factor		
	TBA/EtOH	H_2O/EtOH	ETBE/EtOH	TBA/EtOH	H_2O/EtOH	ETBE/EtOH
1.	0	0	0.0581	0	0	0.5909
2.	0.5873	0	0	0.7520	0	0
3.	0	0.2301	0	0	2.1199	0
4.	1.0294	0.8407	0	0.7434	2.1320	0
5.	0.8700	0.2823	0.0314	0.7432	2.1140	0.6106

For example: Kinetic study

Reaction condition: Catalyst = beta zeolite with Si/Al = 55, catalyst weight = 15 g, $M_{TBA,0}$ = 1.75 mol, $M_{EtOH,0}$ = 1.75 mol, M_{H2O} = 0.10 mol, M_{ETBE} = 0 mol and T= 333 K)

Components	Area	Area ratio	Mole ratio	Mole fraction
EtOH	350737	1	1	0.4437
TBA	455338	1.2982	0.9687	0.4298
H_2O	33433	0.0953	0.2023	0.0897
ETBE	62655	0.1376	0.0827	0.0367

APPENDIX B

UNIFAC CALCULATION

The UNIQUAC equation treats $g \equiv G^E / RT$ as comprised of two additive parts, a *combinatorial* term g^C to account for molecular size and shape differences, and a *residual* term g^R to account for molecular interactions:

$$g = g^C + g^R \tag{B-1}$$

Function g^C contains pure-species parameters only, whereas function g^R incorporates two binary parameters for each pair of molecules. For a multicomponent system,

$$g^C = \sum x_i \ln \frac{\phi_i}{x_i} + 5 \sum q_i x_i \ln \frac{\theta_i}{\phi_i} \tag{B-2}$$

and

$$g^R = -\sum q_i x_i \ln(\sum \theta_j \tau_{ji}) \tag{B-3}$$

where

$$\phi_i = \frac{x_i r_i}{x_j r_j}_i \tag{B-4}$$

and

$$\theta_i = \frac{x_i q_i}{x_j q_j}_i \tag{B-5}$$

Subscript i identifies species, and j is a dummy index; all summations are over all species. Note that $\tau_{ji} \neq \tau_{ii}$; however, when $i = j$, then $\tau_{jj} = \tau_{ii} = 1$. In these equations r_i (a relative molecular volume) and q_i (a relative molecular surface area) are pure-species parameters. The influence of temperature on g enters through the interaction parameters τ_{ji} of Eq.(B-3), which are temperature dependent:

$$\tau_{ji} = exp \frac{-(u_{ji} - u_{ii})}{RT}_i \tag{B-6}$$

Parameters for the UNIQUAC equation are therefore values of $(u_{ji} - u_{ii})$.

An expression for $\ln \gamma_i$ is applied to the UNIQUAC equation for *g* [Eqs.(B-1) through (B-3)]. The result is given by the following equations:

$$\ln \gamma_i = \ln \gamma_i^C + \ln \gamma_i^R \qquad \text{(B-7)}$$

$$\ln \gamma_i^C = 1 - J_i + \ln J_i - 5q_i(1 - \frac{J_i}{L_i} + \ln \frac{J_i}{L_i}) \qquad \text{(B-8)}$$

and

$$\ln \gamma_i^R = q_i(1 - \ln s_i - \sum \theta_j \frac{\tau_{ij}}{s_j}) \qquad \text{(B-9)}$$

where in addition to Eqs. (B-5) and (B-6)

$$J_i = \frac{r_i}{\sum x_j r_j} \qquad \text{(B-10)}$$

$$L_i = \frac{q_i}{\sum x_j q_j} \qquad \text{(B-11)}$$

$$s_i = \sum \theta_l \tau_{li} \qquad \text{(B-12)}$$

again subscript *i* identifies species, and *j* and *l* are dummy indices. All summations are over all species, and τ_{ij} =1 for *i*=*j*. Values for the parameters (u_{ij} - u_{jj}) are found by regression of binary VLE data, and are given by Gmehling et al.

The UNIFAC method for estimation of activity coefficient depends on the concept that a liquid mixture may be considered a solution of the structural units from which the molecules are formed lather than a solution of the molecules themselves. These structural units are called subgroups, and a few of them are listed in the second column of table B.1. A number, designated k, identifies each subgroup. The relative volume R_k and relative surface area Q_k are properties of the subgroups, and values are listed in column 4 and 5 of table B.1. Also shown (Bolumns 6 and 7) are examples of the subgroup compositions of molecular species. When it is possible to construct a molecule from more than one set of subgroups, the set containing the least member of different subgroups id the correct set. The great advantage of the UNIFAC method is

that a relatively small number of subgroups combine to form a very large number of molecules.

Activity coefficients depend not only on the subgroup properties R_k and Q_k, but also on interactions between subgroups. Here, similar subgroups are assigned to a main group, as shown in the first two columns of table B.1. The designations of main groups, such as "CH_2" , "ACH", etc., are descriptive only. All subgroups belonging to the same main group are considered identical with respect to group interactions. Therefore parameters characterizing group interactions are identified with pairs of main groups. Parameter value a_{mk} for a few such pairs are given in table B.2.

The UNIFAC method is base on the UNIQUAC equation, for which the activity coefficients are given by equation B-7. When applied to a solution of groups, Eqs. B-8 and B-9 are written:

$$\ln \gamma_i^{\,C} = 1 - J_i + \ln J_i - 5q_i\left(1 - \frac{J_i}{L_i} + \ln \frac{J_i}{L_i}\right) \qquad \text{(B-13)}$$

and

$$\ln \gamma_i^{\,R} = q_i\left[1 - \sum\left(\theta_k \frac{\beta_{ik}}{s_k} - e_{ki} \ln \frac{\beta_{ik}}{s_k}\right)\right] \qquad \text{(B-14)}$$

The quantities J_i and L_i are still given by Eqs. B-10 and B-11. In addition, the following definition apply:

$$r_i = \sum \nu_k^{(i)} R_k \qquad \text{(B-15)}$$

$$q_i = \sum \nu_k^{(i)} Q_k \qquad \text{(B-16)}$$

$$e_{ki} = \frac{\nu_k^{(i)} Q_k}{q_i} \qquad \text{(B-17)}$$

$$\beta_{ik} = \sum e_{mi} \tau_{mk} \qquad \text{(B-18)}$$

$$\theta_k = \frac{\sum x_i q_i e_{ki}}{\sum x_j q_j} \qquad \text{(B-19)}$$

$$s_k = \sum \theta_m \tau_{mk} \qquad \text{(B-20)}$$

$$\tau_{mk} = \exp \frac{-a_{mk}}{T} \qquad \text{(B-21)}$$

Subscript *i* identifies species, and *j* is a dummy index running over all species. Subscript *k* identifies subgroups, and *m* is a dummy index running over all subgroups. the quantity $\nu_k^{(i)}$ is the number of subgroups of type *k* in a molecule of species *i*. Values of the subgroup parameters R_k and Q_k and of the group interaction parameters a_{mk} come from tabulation in the literature. Tables B.1 and B.2 show a few parameter values; the number designations of the compete table are remained.

Table B.1: UNIFAC-VLE subgroup parameters

Main group	Subgroup	*k*	R_k	Q_k	Examples of molecules and their constituent groups	
1 "CH_2"	CH_3	1	0.9011	0.848	*n*-Butane:	$2CH_3, 2CH_2$
	CH_2	2	0.6744	0.540	Isobutane:	$3CH_3, 1CH$
	CH	3	0.4469	0.228	2,2-Dimethyl	
	C	4	0.2195	0.000	propane:	$4CH_3, 1C$
3 "ACH" (AC = aromatic carbon)	ACH	10	0.5313	0.400	Benzene:	6ACH
4 "$ACCH_2$"	$ACCH_3$	12	1.2663	0.968	Toluene:	$5ACH, 1ACCH_3$
	$ACCH_2$	13	1.0396	0.660	Ethylbenzene:	$1CH_3, 5ACH, 1ACCH_2$
5 "OH"	OH	15	1.0000	1.200	Ethanol:	$1CH_3, 1CH_2, 1OH$
7 "H_2O"	H_2O	17	0.9200	1.400	Water:	$1H_2O$
9 "CH_2CO"	CH_3CO	19	1.6724	1.488	Acetone:	$1CH_3CO, 1CH_3$
	CH_2CO	20	1.4457	1.180	3-Pentanone:	$2CH_3, 1CH_2CO, 1CH_2$
13 "CH_2O"	CH_3O	25	1.1450	1.088	Dimethyl ether:	$1CH_3, 1CH_3O$
	CH_2O	26	0.9183	0.780	Diethyl ether:	$2CH_3, 1CH_2, 1CH_2O$
	CH−O	27	0.6908	0.468	Diisopropyl ether:	$4CH_3, 1CH, 1CH-O$
15 "CNH"	CH_3NH	32	1.4337	1.244	Dimethylamine:	$1CH_3, 1CH_3NH$
	CH_2NH	33	1.2070	0.936	Diethylamine:	$2CH_3, 1CH_2, 1CH_2NH$
	CHNH	34	0.9795	0.624	Diisopropylamine:	$4CH_3, 1CH, 1CHNH$
19 "CCN"	CH_3CN	41	1.8701	1.724	Acetonitrile:	$1CH_3CN$
	CH_2CN	42	1.6434	1.416	Propionitrile:	$1CH_3, 1CH_2CN$

[1]H. K. Hansen, P. Rasmussen, Aa. Fredenslund, M. Schiller, and J. Gmehling, *IEC Research*, vol. 30, pp. 2352–2355, 1991.

Table B.2: UNIFAC-VLE interaction parameters, a_{mk}, in kelvins

	1	3	4	5	7	9	13	15	19
1 CH_2	0.00	61.13	76.50	986.50	1,318.00	476.40	251.50	255.70	597.00
3 ACH	−11.12	0.00	167.00	636.10	903.80	25.77	32.14	122.80	212.50
4 $ACCH_2$	−69.70	−146.80	0.00	803.20	5,695.00	−52.10	213.10	−49.29	6,096.00
5 OH	156.40	89.60	25.82	0.00	353.50	84.00	28.06	42.70	6.712
7 H_2O	300.00	362.30	377.60	−229.10	0.00	−195.40	540.50	168.00	112.60
9 CH_2CO	26.76	140.10	365.80	164.50	472.50	0.00	−103.60	−174.20	481.70
13 CH_2O	83.36	52.13	65.69	237.70	−314.70	191.10	0.00	251.50	−18.51
15 CNH	65.33	−22.31	223.00	−150.00	−448.20	394.60	−56.08	0.00	147.10
19 CCN	24.82	−22.97	−138.40	185.40	242.80	−287.50	38.81	−108.50	0.00

[1]H. K. Hansen, P. Rasmussen, Aa. Fredenslund, M. Schiller, and J. Gmehling, *IEC Research*, vol. 30, pp. 2352–2355, 1991.

APPENDIX C

CALCULATION OF THE SPECIFIC SURFACE AREA

From Brunauer-Emmett-Teller (BET) equation.

$$\frac{p}{n(1-p)} = \frac{1}{n_m C} + \frac{(C-1)p}{n_m C} \qquad (C.1)$$

Where, p = Relative partial pressure of adsorbed gas, P/P_0

P_0 = Saturated vapor pressure of adsorbed gas in the condensed state at the experimental temperature, atm

P = Equilibrium vapor pressure of adsorbed gas, atm

n = Gas adsorbed at pressure P, ml. at the NTP/g of sample

n_m = Gas adsorbed at monolayer, ml. at the NTP/g of sample

C = Exp $[(H_C - H_l)/RT]$

H_C = Heat of condensation of adsorbed gas on all other layers

H_l = Heat of adsorption into the first layer

Assume $C \rightarrow \infty$, then

$$\frac{p}{n(1-p)} = \frac{p}{n_m}$$

$$n_m = n(1 - p) \qquad (C.2)$$

The surface area, S, of the catalyst is given by

$$S = S_b \times n_m \qquad (C.3)$$

From the gas law

$$\frac{P_b V}{T_b} = \frac{P_t V}{T_t} \qquad (C.4)$$

Where, P_b = Pressure at 0°C

P_t = Pressure at t°C

T_b = Temperature at 0°C = 273.15 K

T_t = Temperature at t°C = 273.15 + t K

V = Constant volume

Then, $P_b = (273.15/ T_t) \times P_t = 1$ atm

Partial pressure

$$P = \frac{[\text{Flow of } (He + N_2) - \text{Flow of } He]}{\text{Flow of } (He + N_2)} \quad (C.5)$$

$$= 0.3 \text{ atm}$$

For nitrogen gas, the saturated vapor pressure equals to

$$P_0 = 1.1 \text{ atm}$$

then, $p = P/P_0 = 0.3/1.1 = 0.2727$

To measure the volume of nitrogen adsorbed, n

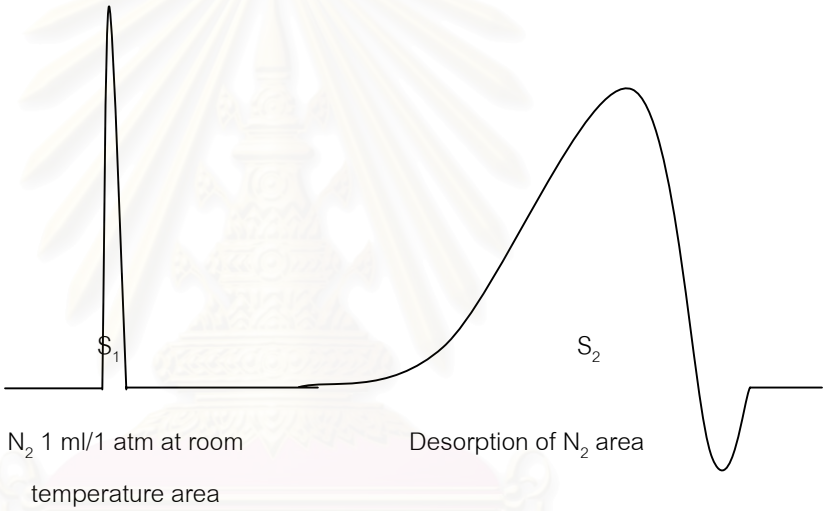

$$n = \frac{S_2}{S_1} \times \frac{1}{W} \times \frac{273.15}{T} \text{ ml. /g of catalyst} \quad (C.6)$$

Where, S_1 = N_2 1 ml/1 atm at room temperature area

S_2 = Desorption of N_2 area

W = Sample weight, g

T = Room temperature, K

Therefore,

$$n_m = \frac{S_2}{S_1} \times \frac{1}{W} \times \frac{273.15}{T} \times (1 - p)$$

$$n_m = \frac{S_2}{S_1} \times \frac{1}{W} \times \frac{273.15}{T} \times 0.7272 \quad (C.2.1)$$

Whereas, the surface area of nitrogen gas from literature equal to

S_b = 4.373 m^2/ml of nitrogen gas

Then,

$$S = \frac{S_2}{S_1} \times \frac{1}{W} \times \frac{273.15}{T} \times 0.7272 \times 4.343$$

$$S = \frac{S_2}{S_1} \times \frac{1}{W} \times \frac{273.15}{T} \times 3.1582 \ m^2/g \qquad \text{(C.7)}$$

VITA

Miss Darin Wongwatttanasat was born on July 26th , 1979 in Nakhon Sawan, Thailand. She received the Bachelor Degree of Science in Industrial Chemistry from Faculty of Science, King Mongkut's Institute of Technology Ladkrabang in 2000. She continued her Master study at Chulalongkorn University in June, 2000.